bioRxiv preprint doi: https://doi.org/10.1101/2020.06.18.159806; this version posted June 18, 2020. The copyright holder for this preprint (which was not certified by peer review) is the author/funder. All rights reserved. No reuse allowed without permission.

Structural basis for phosphorylation independent activation of c-CBL by Src-like adaptor protein 2.

Authors: Leanne E. Wybenga-Groot[abc*], Andrea J. Tench[abd], Craig D. Simpson[ab], Jonathan St. Germain[e], Brian Raught[de], Michael F. Moran[bcf], C. Jane McGlade[abd]*

[a]The Arthur and Sonia Labatt Brain Tumour Research Centre, [b]Program in Cell Biology, [c]SPARC BioCentre, The Hospital for Sick Children, 555 University Avenue, Toronto, ON, Canada, M5G 1X8

[d]Department of Medical Biophysics, University of Toronto, 610 University Avenue, Toronto, ON, Canada, M5G 2M9

[e] Princess Margaret Cancer Centre, University Health Network, Toronto, ON, M5G 1L7

[f] Department of Molecular Genetics, 1 King's College Circle, Toronto ON M5S 1A8

*Corresponding authors: leanne.wybenga-groot@sickkids.ca, 647-822-3897; jmcglade@sickkids.ca, 416-813-8657

Keywords: Src-like adaptor protein, CBL, protein-protein interaction, ubiquitin ligase, X-ray crystal structure, activation mechanism

bioRxiv preprint doi: https://doi.org/10.1101/2020.06.18.159806; this version posted June 18, 2020. The copyright holder for this preprint (which was not certified by peer review) is the author/funder. All rights reserved. No reuse allowed without permission.

Abstract

CBL is a RING type E3 ubiquitin ligase that functions as a negative regulator of tyrosine kinase signaling and loss of CBL function is implicated in several forms of leukemia. The Src-like adaptor proteins (SLAP/SLAP2) bind to CBL and are key components of CBL-dependent downregulation of antigen receptor, cytokine receptor, and receptor tyrosine kinase signaling. To understand the molecular basis of the interaction between SLAP/SLAP2 and CBL, we solved the crystal structure of CBL tyrosine kinase binding domain (TKBD) in complex with SLAP2. The carboxy-terminal region of SLAP2 adopts an α-helical structure which binds in a cleft between the 4H, EF-hand, and SH2 domains of the TKBD. This SLAP2 binding site is remote from the canonical TKBD phospho-tyrosine peptide binding site but overlaps with a region important for stabilizing CBL in its autoinhibited conformation. Addition of SLAP2 to autoinhibited CBL *in vitro* activates CBL autoubiquitination. As well, disruption of the CBL/SLAP2 interface through mutagenesis demonstrates a role for this protein-protein interaction in regulation of CBL E3 ligase activity in cells. Our results reveal that SLAP2 binding provides an alternative mechanism for activation of CBL ubiquitin ligase function.

bioRxiv preprint doi: https://doi.org/10.1101/2020.06.18.159806; this version posted June 18, 2020. The copyright holder for this preprint (which was not certified by peer review) is the author/funder. All rights reserved. No reuse allowed without permission.

Introduction

Ubiquitin (Ub) modification of proteins regulates cellular processes including cell cycle, DNA repair, endocytosis, and signal transduction. The ubiquitination machinery consists of a cascade of E1, E2, and E3 components, which activate and transfer ubiquitin to substrates in a sequential manner[1,2]. Substrate specificity in the ubiquitin system is determined through a large and diverse family of E3 ubiquitin ligases that bind target proteins [3,4]. The Casitas B-cell lymphoma (*CBL*) gene encodes the E3 ubiquitin ligase CBL (also referred to as c-CBL), a central regulator of tyrosine kinase (TK) signaling [5-9]. Ubiquitination of activated receptor TKs by CBL nucleates the assembly of endocytic proteins both at the membrane and at sorting endosomes to promote lysosome targeting, degradation and signal termination[10,11]. CBL is also important for down regulation of signaling from antigen and cytokine receptors through ubiquitination of receptor chains and associated cytosolic TKs, leading to inactivation and/or proteosomal degradation [12-14].

CBL consists of an amino-terminal tyrosine kinase binding domain (TKBD), a linker helix region (LHR) and a really interesting new gene (RING) domain, followed by a carboxy-terminal region containing binding sites for Src homology 2 (SH2) and Src homology 3 (SH3) domain containing signaling and adaptor proteins[7]. CBL TKBD is composed of a four-helix bundle (4H), an EF-hand, and a variant SH2 domain, which binds substrates, such as activated TKs, in a phospho-tyrosine dependent manner [15]. The CBL RING domain binds E2 conjugating enzymes required for ubiquitin transfer to TKBD bound substrates[9,16,17]. Recruitment of CBL to activated TK complexes leads to phosphorylation at a conserved tyrosine residue (Tyr371) within the CBL LHR, and activation of its E3 ligase function[16,18,19]. Structural studies have shown that unphosphorylated CBL adopts a closed autoinhibited conformation with Tyr371

bioRxiv preprint doi: https://doi.org/10.1101/2020.06.18.159806; this version posted June 18, 2020. The copyright holder for this preprint (which was not certified by peer review) is the author/funder. All rights reserved. No reuse allowed without permission.

forming part of a LHR-TKBD interface[20,21]. Phosphorylation of Tyr371 releases the LHR-TKBD interaction causing a conformational change that places the E2 active site in close proximity to TKBD bound substrate, and stabilizing E2 bound ubiquitin for transfer [21,22].

Mutations in *CBL* which impair E3 ligase activity have been identified in juvenile myelomonocytic leukemia (JMML), chronic myelomonocytic leukemia (CMML), and chronic myeloid leukemia (CML), as well as in patients with several other myeloproliferative neoplasms [5,23-28]. Understanding CBL autoinhibition and phosphorylation-dependent activation provide insight into how mutations identified in leukemias can abrogate CBL E3 ligase activity. In addition to mutations in the RING domain, the LHR, and Tyr371 in particular, are frequent targets of missense mutations that prevent phosphorylation dependent activation of CBL ubiquitin ligase function [21,23,24,26]. These mutant forms of CBL are also thought to act through a gain-of-function mechanism, since adaptor functions are retained, allowing signaling protein recruitment through multiple carboxy-terminal SH2 and SH3 binding motifs [29,30].

Src-like adaptor proteins (SLAP and SLAP2) bind CBL and play important roles in CBL activity and regulation of antigen receptor, cytokine receptor, and RTK signaling [31-39]. Both *Cbl* and *Slap* deficient mice have increased T and B cell receptor (TCR and BCR) levels, accompanied by enhanced signaling and positive selection of thymocytes [31,34,35]. *Slap/Slap2* deficient mice also show defective down regulation of Granulocyte/macrophage colony-stimulating factor receptor (GM-CSFR) signaling leading to a block in normal dendritic cell development[40], as well as enhanced platelet activation signaling and arterial thrombus formation[41]. In addition, SLAP/SLAP2 overexpression or depletion in hematopoietic cell lines affects the down regulation of several RTKs, including CSF-1R, c-Kit and FLT3 [42-44,45] . Outside

bioRxiv preprint doi: https://doi.org/10.1101/2020.06.18.159806; this version posted June 18, 2020. The copyright holder for this preprint (which was not certified by peer review) is the author/funder. All rights reserved. No reuse allowed without permission.

the hematopoietic system, SLAP is important for down regulation of SRC and EPHA2 signaling in intestinal epithelial cells as well as PDGFR signaling induced dorsal ruffle formation [46-48].

SLAP and SLAP2 are membrane associated proteins by virtue of an amino-terminal myristoylation site. They contain adjacent SH3 and SH2 domains most closely related to those found in SRC family kinase HCK, followed by a carboxy (C)-terminal tail region lacking obvious domains or protein interaction motifs [33,43,49-51]. The SLAP2 SH3/SH2 domains adopt typical folds with a uniquely short connector sequence that positions them in close association consistent with a functional unit that binds proteins through tandem association [51,52]. SLAP/SLAP2 recruitment to activated receptor TKs is mediated through the SH3/SH2 module, while the C-terminal tail region of both SLAP and SLAP2 constitutively associates with CBL [32,35,53]. SLAP association with CBL is important for ubiquitin dependent down regulation of ZAP-70 and TCRζ, as well as RTKs FLT3 and c-KIT [31,33,35,40,43-45,54].

While CBL binds to multiple SH2 and SH3 domain containing adaptor proteins through canonical binding motifs found in the CBL carboxy-terminal region, SLAP and SLAP2 binding requires a region of the SLAP/SLAP2 C-terminal tail and the CBL TKBD [33,49,50]. Nevertheless, SLAP/SLAP2 binding to CBL is distinct from other TKBD binding proteins as it is independent of tyrosine phosphorylation and is not disrupted by a CBL Gly306Glu mutation, which abolishes TKBD binding to tyrosine phosphorylated substrates [33]. To understand the molecular basis of this interaction, we solved the X-ray crystal structure of CBL TKBD in complex with SLAP2. We describe how a C-terminal region of SLAP2 adopts an α-helical structure that binds CBL TKBD in the same cleft that is occupied by the LHR in the autoinhibited CBL conformation. Furthermore, we find that SLAP2 binding can stimulate CBL autoubiquitination activity

bioRxiv preprint doi: https://doi.org/10.1101/2020.06.18.159806; this version posted June 18, 2020. The copyright holder for this preprint (which was not certified by peer review) is the author/funder. All rights reserved. No reuse allowed without permission.

independent of phosphorylation indicating that in addition to its adaptor functions, SLAP/SLAP2 binding contributes to CBL activation.

bioRxiv preprint doi: https://doi.org/10.1101/2020.06.18.159806; this version posted June 18, 2020. The copyright holder for this preprint (which was not certified by peer review) is the author/funder. All rights reserved. No reuse allowed without permission.

Results

Crystal structure of CBL TKBD in complex with SLAP2

SLAP2 interacts with the CBL TKBD via a phosphorylation independent mechanism involving its C-terminal region (Fig. 1A) [33,53,55]. To understand the molecular basis of this interaction, CBL TKBD and SLAP2 proteins (residues 25-357 and 28-261, respectively) were purified by affinity and size exclusion chromatography. To form a complex of CBL TKBD and SLAP2 for co-crystallization studies, the purified proteins were mixed in a 1:1 molar ratio and subjected to size exclusion chromatography. The proteins eluted as two peaks, one at an earlier volume than typically observed for either CBL TKBD or SLAP2, indicating higher molecular weight (Supplementary Fig. 1A). As confirmed by SDS-PAGE of chromatography fractions, the first peak contained a CBL/SLAP2 complex (Supplementary Fig. 1B), which was concentrated and used for sparse matrix crystallization experiments. Small rod-like crystals diffracted to 2.5 Å resolution, but structure determination by molecular replacement using native CBL TKBD (PDB ID: 2Y1M) and SLAP2 SH3-SH2 (PDB ID: 4M4Z) as models proved unsuccessful, as no solution was found for SLAP2. Using CBL TKBD as a model resulted in a traceable electron density map and refineable model of CBL TKBD. Comparison of the CBL TKBD structure to published or released CBL models in the protein data bank (PDB) revealed no significant changes in overall conformation or secondary structure. However, it was noted that our model of CBL represented a novel mode of configuration or packing of CBL molecules in the crystal asymmetric unit (ASU) (Supplementary Fig. 2A, B). Close examination of the interface between the two CBL molecules in the ASU revealed unassigned electron density that clearly resembled two alpha helices (Supplementary Fig. 2C, D). We reasoned that this density likely represented a portion of SLAP2.

bioRxiv preprint doi: https://doi.org/10.1101/2020.06.18.159806; this version posted June 18, 2020. The copyright holder for this preprint (which was not certified by peer review) is the author/funder. All rights reserved. No reuse allowed without permission.

To identify which residues to assign to the helical electron density, iterative rounds of model refinement and data processing were employed, resulting in improved electron density maps with recognizable side chain densities. Based on observation that the C-terminal tail of SLAP2, excluding residues 198-229 and 255-261, is necessary for CBL binding *in vitro* (Fig. 1B; [33,55]), the fact that large portions of the SLAP2 C-terminal tail are expected to be disordered by secondary structure prediction programs (Fig. 1C) [56], and the contour of the electron density, residues 237-255 of SLAP2 were manually placed into each helix of the unassigned density (Fig. 2A). The resulting model refined readily with good quality refinement statistics (Table 1) signifying that a structure of CBL TKBD in complex with SLAP2 had been determined (Fig. 2B). It was not possible to establish if additional SLAP2 residues co-crystallized with CBL TKBD but remained disordered. However, based on protein packing within the crystal (Supplementary Fig. 2E, F) and our observation that SLAP2 is susceptible to degradation, we conjecture that CBL/SLAP2 co-crystallized following degradation of the C-terminal tail from the SH3-SH2 domain, and that residues 237-255 represent the critical component for CBL/SLAP2 interaction.

Superposition of CBL/SLAP2 with native CBL TKBD (PDB id: 1B47) indicates that CBL adopts the typical integrated module, composed of a calcium-bound EF-hand wedged between a four-helix bundle (4H) and a divergent SH2 domain, with root mean square deviation (rmsd) of 0.9 Å (main chain atoms) for CBL TKBD [15](Fig. 2C). Superposition of the 4H bundle and EF-hand of CBL/SLAP2 with those of native and liganded CBL TKBD (PDB id: 2CBL) shows that binding of the C-terminal portion of SLAP2 to CBL does not induce closure of the domains to the extent that phosphopeptide binding to the SH2 domain does, such that CBL/SLAP2 most resembles unliganded CBL TKBD (Fig. 2C) [15].

bioRxiv preprint doi: https://doi.org/10.1101/2020.06.18.159806; this version posted June 18, 2020. The copyright holder for this preprint (which was not certified by peer review) is the author/funder. All rights reserved. No reuse allowed without permission.

Structure of CBL/SLAP2 defines a novel binding interface

SLAP2 binds as an α-helix in a cleft formed by the three subdomains of TKBD, opposite the phospho-tyrosine peptide binding pocket (Fig. 3A). The SLAP2 binding cleft is framed by helices αC and αD of the 4H bundle, helix αE2 and loop αE2-αF2 of the EF-hand, and helix αN, loop αN-βA, and strand βA of the SH2 domain [15] (Fig. 3A). The CBL/SLAP2 interface is stabilized by hydrophobic interactions involving side chains from Leu241, Leu245, and Leu251 of SLAP2 and Lys153, Leu154, Met222, Ala223, Trp258, and Val263 of CBL, and by hydrogen bonds involving both backbone carbonyl groups and side chain atoms (see Supplementary Table 1 and Supplementary Fig. 3). Altogether, the interaction between CBL and SLAP2 results in 4592 $Å^2$ of overall contact area. The crystal ASU contains two CBL TKBD molecules and two SLAP2 molecules related by a two-fold symmetry axis to form a CBL/SLAP2 dimer (Fig. 2B). The CBL TKBD structure is well ordered except for the N-terminal (25-47 molecule 1, 25-51 molecule 2) and C-terminal (353-357 molecule 1, 352-357 molecule 2) residues. The SLAP2 α-helices interact expansively, stabilized by extensive hydrogen bonding and hydrophobic interactions, while few interactions are formed between the CBL monomers (Supplementary Tables 2 and 3).

To validate the CBL/SLAP2 binding interface, a series of mutants in a Duet co-expression vector system was generated for co-purification trials. The SLAP2 sequence was preceded by thioredoxin (Trx) and His-tag fusion proteins to allow co-purification of CBL TKBD that was bound to Trx-His-SLAP2 during the initial affinity chromatography purification step. Surface residues deemed to be important to the CBL/SLAP2 interface, but not CBL function or folding, were mutated to disrupt CBL/SLAP2 binding (Fig. 3C and Supplementary

bioRxiv preprint doi: https://doi.org/10.1101/2020.06.18.159806; this version posted June 18, 2020. The copyright holder for this preprint (which was not certified by peer review) is the author/funder. All rights reserved. No reuse allowed without permission.

Fig. 3). In our structure, SLAP2 Gly240 locates close to CBL Met269 and Ala270, such that mutation to a bulky Arg residue (G240R) could cause sterical constraints. Similarly, SLAP2 Leu241 is situated in a hydrophobic cleft composed of CBL Ala223, Trp258, and Val263; mutation to Arg (L241R) was predicted to disturb this binding pocket. Mutation of CBL Ala223 to Arg (*A223R*) would likewise disrupt this pocket, with CBL/SLAP2 double mutant *A223R*/L241R predicted to drastically disturb binding through sterical constraints and charge repulsion. (For clarity, CBL mutations herein are indicated in italics, SLAP2 in regular font.) Similarly, single or double mutation of CBL Ser226 or SLAP2 Ser244, whose side chain hydroxyl groups are in close proximity to one another, to charged Glu residues (*S226E* and S244E) was anticipated to interfere with CBL/SLAP2 binding. Finally, given that SLAP2 binds CBL as an α-helix, mutation of Leu245, located in the center of this α-helix, to proline (L245P) was expected to interrupt the helical structure and thus prevent SLAP2 binding. CBL TKBD co-purified with SLAP2 in high salt conditions (0.5 M NaCl), while mutation of either SLAP2 or CBL at interface residues resulted in loss of CBL co-purification (Fig. 3D, upper panel). Co-purification in less stringent low salt concentration (0.15 M NaCl) revealed that mutation at L241R, L245P, and *S226E* still abrogated CBL co-purification, while G240R, S244E, and *A223R* mutations were tolerated, resulting in CBL co-purification (Fig. 3D, lower panel). However, double mutation of the CBL/SLAP2 interface (*A223R*/L241R and *S226E*/S244E; Fig. 3D, lower panel) was not tolerated, even at low salt concentration. In contrast, mutation of SLAP2 residues involved in the SLAP2/SLAP2 interface but not CBL binding (R242A, I249W, S246/250E) did not significantly impact co-purification of CBL, suggesting that TKBD binding does not require a SLAP2 dimer (Fig. 3E).

bioRxiv preprint doi: https://doi.org/10.1101/2020.06.18.159806; this version posted June 18, 2020. The copyright holder for this preprint (which was not certified by peer review) is the author/funder. All rights reserved. No reuse allowed without permission.

The related adaptor protein SLAP also interacts with CBL TKBD [50], and its amino acid sequence corresponding to the SLAP2 C-terminal α-helical region is highly conserved (Fig. 1C). To determine if SLAP binds CBL TKBD by a similar mechanism, we tested SLAP and a set of analogous interface mutants in co-purification experiments. Like SLAP2, SLAP mutations at L241R and I245P abrogated CBL co-purification, while mutations G240R and S224E were tolerated (Fig. 3F). Together, these studies indicate that SLAP and SLAP2 interact with CBL via an α-helix near their C-terminus, which binds to a cleft of the CBL TKBD that is distinct from the canonical phospho-tyrosine binding site in the CBL SH2 domain.

Further examination of the SLAP/SLAP2 α-helix protein sequence revealed a conserved tyrosine residue (Tyr248) (Fig. 1C) that is predicted to be phosphorylated by the Kinexus phosphorylation site prediction algorithm, but to our knowledge has not been experimentally confirmed (www.phosphonet.ca). SLAP2 has been shown to be tyrosine phosphorylated in CSF-1 stimulated FD-Fms cells[42]. To identify SLAP2 tyrosine phosphorylation sites, purified SLAP2 protein was incubated *in vitro* with EphA4 kinase in the presence of ATP. Phosphorylated SLAP2 was detected by an upward shift in molecular weight by SDS-PAGE and confirmed by immunoblot analysis (Fig. 4A). Sites of phosphorylation were identified by in-gel protease digestion of the isolated, shifted band followed by liquid chromatography tandem mass spectrometry (LC-MS/MS), which identified Tyr248 as a site of phosphorylation (Fig. 4B,C). To investigate whether phosphorylation of Y248 impacts SLAP2 binding to CBL, co-purification experiments were performed under conditions where SLAP2 was tyrosine phosphorylated. CBL TKBD co-purified with phosphorylated SLAP2 WT and Y248F indicating that SLAP2 interaction with CBL is not disrupted by Y248 phosphorylation, nor is it required for binding (Fig. 4D). In agreement, a phosphate ion was modeled on the side chain hydroxyl of Tyr248 in

bioRxiv preprint doi: https://doi.org/10.1101/2020.06.18.159806; this version posted June 18, 2020. The copyright holder for this preprint (which was not certified by peer review) is the author/funder. All rights reserved. No reuse allowed without permission.

the CBL/SLAP2 structure (Fig. 4E). The structure appears to accommodate phosphorylation at Tyr248 without causing sterical constraints at the CBL/SLAP2 interface.

SLAP2 binding to CBL precludes inhibitory LHR-RING interactions with the TKBD

Unphosphorylated CBL adopts a closed, autoinhibited conformation in which the LHR and RING domain pack against the TKBD in a manner that restricts ubiquitin ligase activity [20,21]. Phosphorylation of Tyr371 in the LHR disrupts these interactions, reorients the LHR-RING in proximity of substrates, and stabilizes E2 bound ubiquitin for transfer [21,22]. Superposition of CBL/SLAP2 with structures of autoinhibited CBL (TKBD-LHR-RING, PDB id:2Y1N and TKBD-LHR-RING plus E2, PDB id:1FBV) revealed that SLAP2 binds to a similar region of CBL TKBD as the regulatory LHR and RING domain (Fig. 5A,B). The LHR forms an ordered loop and an α-helix that pack against the TKBD, with linker-TKDB interactions centered on linker residues Tyr368 and Tyr371 [20]. In the CBL/SLAP2 structure, SLAP2 residue Leu241 occupies the same buried environment as Tyr371 in autoinhibited CBL (Fig. 5C). Moreover, side chain residues from helix αE2 of the EF-hand, such as Ala223 and Ser226, as well as Val263 from loop αN-βA of the SH2 domain, make multiple van der Waals contacts with the linker helix in autoinhibited CBL; these same residues are involved in the SLAP2 binding site (Fig. 3C, Supplementary Fig. 3, Supplementary Table 1). Similarly, the SLAP2 α-helix and its C-terminal extension occupy the same space as linker-loop 2 of the LHR and the N-terminus of the RING domain in closed CBL, respectively (Fig. 5C). Indeed, several residues which stabilize the TKBD-RING interface in closed CBL, including Gln128, Asn150, Lys153, and Leu154, are involved in SLAP2 binding in the CBL/SLAP2 structure (Supplementary Fig. 3, Supplementary

bioRxiv preprint doi: https://doi.org/10.1101/2020.06.18.159806; this version posted June 18, 2020. The copyright holder for this preprint (which was not certified by peer review) is the author/funder. All rights reserved. No reuse allowed without permission.

Table 1). CBL residue Met222 stabilizes the TKBD-RING interface in autoinhibited CBL and forms part of an E2 binding pocket upon the addition of UbcH7 [20,21]. Notably, Met222 is also involved in hydrophobic interactions with Leu245 and Ile249 of the SLAP2 α-helix. These observations suggest a model in which SLAP2 binding to CBL would preclude LHR-RING interactions with the TKBD and favour the open, catalytically competent conformation (Fig. 5D).

CBL TKBD binding to SLAP2 promotes ubiquitin ligase activity

Given that binding of SLAP2 and the LHR-RING would be mutually exclusive (Fig. 5C), we reasoned that binding of SLAP2 to CBL could displace the LHR-RING, thereby promoting the catalytically competent conformation (Fig. 5D). To test this hypothesis, an *in vitro* ubiquitination assay in which E3 ligase activity is detected by a smear at high molecular weight on an anti-ubiquitin (Ub) immunoblot was employed [9,19]. As previously reported, purified CBL TKBD-LHR-RING (2-436) had no detectable ubiquitination activity, while its phosphorylated version (pCBL) displayed substantial activity, indicating the inactive and active forms of CBL, respectively (Fig. 6A) [19]. Addition of purified SLAP2 or phosphorylated SLAP2 (pSLAP2) to unphosphorylated CBL stimulated CBL ubiquitination activity *in vitro* (Fig. 6A). Notably, addition of pSLAP2 to CBL appeared to promote CBL ubiquitination activity to a greater extent than addition of SLAP2 (Fig. 6A,B). Neither addition of SLAP2 nor pSLAP2 to active pCBL appeared to further enhance or diminish ubiquitination activity (Fig. 6A). To further compare and quantify CBL ubiquitin ligase activity, a chemiluminescence based assay which measures the total amount of polyubiquitylated products formed in an *in vitro* reaction was used. In this assay, production of polyubiquitylated proteins increased upon addition of SLAP2 or pSLAP2 to

bioRxiv preprint doi: https://doi.org/10.1101/2020.06.18.159806; this version posted June 18, 2020. The copyright holder for this preprint (which was not certified by peer review) is the author/funder. All rights reserved. No reuse allowed without permission.

CBL, compared to CBL alone (Fig. 6C and Supplementary Fig. 4A). Consistent with the anti-Ub immunoblot analysis, pSLAP2 stimulated CBL ligase activity to a greater extent than SLAP2. Notably, the ubiquitin ligase activity of CBL/pSLAP2 remained far less than that of pCBL (Fig. 6A,C). This suggests that pSLAP2 interaction with CBL is partially activating, such that a catalytically competent conformation is favoured upon SLAP2 binding (Fig. 5D).

Ubiquitin contains seven internal lysine residues (K6, K11, K27, K29, K33, K48 and K63) that can be modified with additional Ub molecules to form extended oligomers or "chains" [2,57]. To further examine the impact of pSLAP2 on CBL ubiquitination activity, we determined the type of Ub linkages generated *in vitro* by pCBL or CBL in the presence of SLAP2 or pSLAP2, as different types of Ub chains can confer different biological outcomes. Reactions from the *in vitro* ubiquitination assay were analyzed by LC-MS/MS. Mass spectrometry data was searched against the human proteome, with diglycine as a variable modification on lysine, and the MS1 peak area corresponding to each linkage type quantified [57]. Phosphorylated CBL generated predominantly K48 linked Ub chains with smaller proportions of K11 and K63 linkages (Fig. 6D). Similar proportions of Ub chain linkages were observed when unphosphorylated CBL was incubated with either SLAP2 or pSLAP2 (Fig. 6D) indicating that the *in vitro* ubiquitination activity of CBL in the presence of SLAP2 or pSLAP2 is similar to that of phosphorylated CBL.

To assess the specific role of SLAP2 α-helix in CBL activation, we tested the ability of SLAP2 mutants L241R and S244E to promote CBL ligase activity. Phosphorylated SLAP2 L241R exhibited reduced stimulation of CBL ubiquitination activity compared to pSLAP2 WT (Fig. 7A,B and Supplementary Fig. 4B). Phosphorylated SLAP2 S244E, which maintained CBL binding under low salt conditions (Fig. 3D) such as those used in the ubiquitination assay, also

bioRxiv preprint doi: https://doi.org/10.1101/2020.06.18.159806; this version posted June 18, 2020. The copyright holder for this preprint (which was not certified by peer review) is the author/funder. All rights reserved. No reuse allowed without permission.

exhibited less stimulation of CBL ubiquitination activity than pSLAP2 WT (Fig. 7A,B and Supplementary Fig. 4B). In contrast, SLAP2 mutants R242A, I249W, and S246/250E, which do not interfere with CBL/SLAP2 binding but are predicted to disrupt the dimer interface of SLAP2 α-helices observed in our structure, did not alter SLAP2 or pSLAP2 activation of CBL (Supplementary Fig. 4C,D). This suggests that activation of CBL by SLAP2 requires binding of the SLAP2 C-terminal tail α-helix to the CBL TKBD surface identified in the CBL/SLAP2 crystal structure. Given this CBL interface is also involved in maintaining CBL in an inactive state, through interactions with its LHR and RING domain, we refer to this region as the CBL regulatory cleft.

Engagement of tyrosine phosphorylated substrates by CBL TKBD leads to reorientation of the RING domain and consequently increased E2 binding [21]. Thus, we tested whether the ability of SLAP2 to promote CBL ubiquitination activity is influenced by canonical TKBD-phospho-tyrosine interactions. CBL mutant *G306E*, which abolishes phospho-tyrosine binding *in vitro* [15,33], behaved similarly to WT CBL in ubiquitination assays, such that pSLAP2 also stimulated CBL *G306E* ubiquitination activity (Fig. 7C,D and Supplementary Fig. 4E). This indicates that SLAP2 activation of CBL is independent of both CBL Tyr371 phosphorylation and an intact CBL TKBD substrate binding domain.

Disruption of the SLAP2 binding TKBD regulatory cleft promotes CBL substrate ubiquitination

Next, the ubiquitination activity of CBL proteins mutated in the CBL regulatory cleft was compared to CBL WT. Strikingly, mutations *A223R*, *S226E*, and *A223R/S226E* (*AR/SE*) lead to activation of unphosphorylated CBL, compared to WT, suggesting that mutations in the SLAP2

bioRxiv preprint doi: https://doi.org/10.1101/2020.06.18.159806; this version posted June 18, 2020. The copyright holder for this preprint (which was not certified by peer review) is the author/funder. All rights reserved. No reuse allowed without permission.

binding cleft also disrupt the interaction between CBL TKBD and the LHR (Fig. 8A,B and Supplementary Fig. 4F). These data indicate that mutations of CBL which disrupt SLAP2 binding may also disrupt the autoinhibitory LHR-TKBD interaction and confer phosphorylation independent activation.

To investigate the role of CBL/SLAP2 interaction in cells, the effect of the CBL *A223R/S226E* mutation on substrate binding and ubiquitination was examined. First, to confirm that the *AR/SE* mutation does not disrupt TKBD folding and binding to phospho-tyrosine substrates, glutathione-S-transferase (GST)-tagged WT or mutant CBL TKBD-LHR-RING fusion proteins were isolated on beads and incubated with lysates from COS-7 cells stimulated with epidermal growth factor (EGF). Captured proteins bound to either CBL WT or regulatory cleft mutants were analyzed by anti-EGF receptor (EGFR) immunoblot (Fig. 8C). CBL regulatory cleft mutants *A223R*, *S226E* and *AR/SE* all retained the ability to bind activated EGFR, indicative of functional TKBD phospho-tyrosine binding, whereas the SH2 mutant *G306E* did not bind EGFR. Next, the *A223R/S226E* mutation was introduced into full length HA-tagged CBL and co-transfected into HEK293 cells with His-Ub and FLAG-tagged EGFR. Protein lysates from cells expressing CBL *AR/SE* showed enhanced incorporation of His-Ub compared to cells expressing CBL WT (Fig, 8D) with or without EGFR co-expression. Furthermore, ubiquitination of immunoprecipitated EGFR was increased when co-expressed with CBL *AR/SE* compared to CBL WT (Fig. 8E,F). Together these data support a role for SLAP2 binding and the TKBD regulatory cleft in promoting CBL ubiquitination of TK substrates.

bioRxiv preprint doi: https://doi.org/10.1101/2020.06.18.159806; this version posted June 18, 2020. The copyright holder for this preprint (which was not certified by peer review) is the author/funder. All rights reserved. No reuse allowed without permission.

bioRxiv preprint doi: https://doi.org/10.1101/2020.06.18.159806; this version posted June 18, 2020. The copyright holder for this preprint (which was not certified by peer review) is the author/funder. All rights reserved. No reuse allowed without permission.

Discussion

Compared to other phospho-tyrosine binding domains such as PTB and SH2 domains, the more complex architecture of CBL TKBD could provide additional protein interaction sites and regulatory regions[15]. Indeed, the CBL/SLAP2 structure reveals the presence of an additional intermolecular protein interaction surface formed by regions of the SH2 domain, EF-hand and four-helix bundle that is distinct from the phospho-tyrosine binding site. While other adaptor proteins shown to bind CBL TKBD, such as APS and Sprouty, are phospho-tyrosine and SH2 domain dependent, SLAP2 binding involves a unique surface of TKBD and does not require SLAP2 tyrosine phosphorylation[58-60].

CBL E3 ligase function is integral to regulation of tyrosine kinase signaling through ubiquitination of tyrosine phosphorylated substrates. Furthermore, CBL activity is controlled by tyrosine phosphorylation which regulates the equilibrium between the autoinhibited and catalytically open conformational states [21]. Our study reveals that SLAP/SLAP2 adaptor binding provides an additional mechanism to regulate CBL E3 ligase activity. The structure of SLAP2 bound to CBL TKBD showed that the SLAP2 binding site overlaps the region bound by the LHR in the autoinhibited conformation [21]. Therefore, SLAP2 adaptor binding could hinder access to the closed conformation, shifting the equilibrium toward the activated state. Indeed, addition of SLAP2 promoted CBL ubiquitin ligase activity *in vitro*. However, SLAP2 binding did not stimulate CBL activity to the same magnitude as phosphorylation of CBL at Tyr371. This suggests that the effect of SLAP2 binding on the equilibrium between closed and open conformations is dynamic, presumably due to the absence of phosphorylated LHR residue Tyr371, which serves to stabilize the active conformation of CBL[21]. While the aromatic ring of pTyr371 forms hydrophobic interactions with other LHR residues in active CBL, the phosphate

bioRxiv preprint doi: https://doi.org/10.1101/2020.06.18.159806; this version posted June 18, 2020. The copyright holder for this preprint (which was not certified by peer review) is the author/funder. All rights reserved. No reuse allowed without permission.

moiety forms crucial hydrophilic interactions with Lys382 and Lys389 of the RING domain [21]. Therefore, SLAP2 interaction with CBL would favor an open catalytically competent conformation, but lacks the pTyr371 interactions with the RING domain that stabilize E2 bound ubiquitin for transfer and optimize k_{cat} for CBL autoubiquitination[21,22].

It remains unclear why phosphorylation of SLAP2 Y248, although not required for binding to TKBD, lead to more robust CBL activation *in vitro*. Since Y248 resides within the region that binds the TKBD, phosphorylation at Y248 may stabilize the SLAP2 α-helix or facilitate order transition within the SLAP2 carboxy-terminal region, as observed for numerous signaling proteins [61,62]. Phosphorylation at Y248 may also increase the affinity of SLAP2 for CBL, thus displacing the LHR from the autoinhibited conformation more efficiently. Assessment of binding affinity through standard approaches have been hindered due to the hydrophobic and linear nature of corresponding synthetic peptides and the instability and insolubility of purified SLAP2 proteins at concentrations and conditions required for quantitative binding assays. As well, it is possible that phosphorylation at Y248 results in allosteric regulation of CBL activity or impacts how full-length SLAP2 protein interacts with CBL. Additional investigation will be needed to address the dynamic conformational changes in CBL TKBD-LHR-RING induced by SLAP2 and pSLAP2 proteins.

Three mammalian CBL proteins are encoded by separate genes: CBL (also known as c-Cbl and studied here), Cbl-b, and Cbl-c [63]. CBL and CBL-b proteins are highly homologous in the TKBD and Cbl-b is also regulated by phosphorylation of LHR tyrosine residue (Y363), which relieves autoinhibition to enhance ubiquitin ligase activity [21,22,64,65]. The residues involved in SLAP2 binding as identified by our CBL/SLAP2 crystal structure are conserved in Cbl-b

bioRxiv preprint doi: https://doi.org/10.1101/2020.06.18.159806; this version posted June 18, 2020. The copyright holder for this preprint (which was not certified by peer review) is the author/funder. All rights reserved. No reuse allowed without permission.

TKBD and SLAP has been shown to bind Cbl-b *in vitro* [66]. Therefore, SLAP binding may also provide a mechanism for phosphorylation independent activation of Cbl-b.

Protein-protein interactions as a means to regulate activity has previously been observed for E3 ligases, including CBL family proteins. Cbl-c ubiquitination activity is increased by interaction of its RING finger domain with a LIM domain of Hic-5, a member of the paxillin family [67]. However, in contrast to our observations for activation of CBL by SLAP2 binding, Hic-5 can increase the activity of Cbl-c only after the E3 is activated by phosphorylation or phosphomimetic mutation at LHR Y341 [67]. The HECT E3 Smurf2 also adopts an autoinhibited structure that is relieved by binding an adaptor protein, Smad7 [68,69]. Smad7 regulates the ubiquitin ligase activity of Smurf2 by promoting E2 binding to the HECT domain [68]. Thus, adaptor protein binding as a means to regulate E3 activity may be a more general mechanism [70,71].

Our data help explain the requirement for SLAP/SLAP2 adaptor proteins in CBL dependent down-regulation of TK signaling. Analysis of SLAP deficient mice have highlighted its involvement in T and B cell development, dendritic cell maturation, platelet activation and mast cell degranulation [34,40,41,66,72]. The phenotypes observed were shown to be a consequence of defective down regulation of tyrosine kinase linked receptors including TCR, BCR, GM-CSFR[34,40,72]. In addition, studies in cell lines have demonstrated that the SLAP/SLAP2 C-terminus is required for CBL dependent down regulation of TCR and BCR as well as receptor tyrosine kinases such as CSF-1R and FLT3 [33,35,36,42,43,45,53,73]. These studies have suggested that SLAP/SLAP2 adaptor function has a role in the recruitment of CBL to activated tyrosine kinase complexes, facilitating phosphorylation and proximity to substrates. Our results reveal a more complex role in which the SLAP/SLAP2 C-terminal region binding to CBL TKBD also regulates

bioRxiv preprint doi: https://doi.org/10.1101/2020.06.18.159806; this version posted June 18, 2020. The copyright holder for this preprint (which was not certified by peer review) is the author/funder. All rights reserved. No reuse allowed without permission.

ubiquitin ligase activity. Developmentally regulated and cell type specific expression of SLAP/SLAP2, therefore, could promote CBL activity in specific cellular contexts [37,39,43] .

SLAP/SLAP2 binding to CBL would allow the ubiquitination of substrates in the absence of CBL activation mediated by tyrosine phosphorylation. Such a mechanism could contribute to the constitutive ubiquitination of TCR CD3ζ chain in double positive (DP) thymocytes that occurs during T-cell development. A prior study demonstrated that MHC-independent tonic ubiquitination of the TCR:CD3 complex requires both CBL and SLAP and coincides with the timing of upregulated SLAP expression in DP thymocytes [34,74]. In this context, SLAP binding may serve to promote ubiquitination of substrates in the absence of activated TK signaling and CBL tyrosine phosphorylation by favoring the catalytically competent conformation. Alternatively, in the presence of an activated tyrosine kinase, SLAP/SLAP2 binding and displacement of the TKBD bound LHR might facilitate Y371 phosphorylation and lower the threshold for CBL activation.

In addition to the role of the SLAP/SLAP2 carboxy-terminal tail in CBL ubiquitin ligase activity, binding induced conformational changes in CBL may also influence substrate selection, as well as protein-protein interactions related to CBL adaptor function. Although we did not observe any differences in ubiquitin chain linkages assembled by phosphorylated CBL or SLAP bound CBL *in vitro*, it is possible that distinct mechanisms of activation could influence substrate ubiquitination qualitatively, resulting in distinct protein fates. In addition, the open conformation induced by SLAP/SLAP2 binding may be similar to that imposed by some LHR mutations which allow RING flexibility and ubiquitination of substrates bound to regions distinct from TKBD phospho-tyrosine substrate binding pocket[75]. Together, our observations suggest

bioRxiv preprint doi: https://doi.org/10.1101/2020.06.18.159806; this version posted June 18, 2020. The copyright holder for this preprint (which was not certified by peer review) is the author/funder. All rights reserved. No reuse allowed without permission.

that SLAP/SLAP2 binding to CBL could provide a mechanism to tune CBL activity or substrate selection in the context of different degrees of tyrosine kinase signaling.

In conclusion, our results reveal a novel phosphorylation independent protein-protein interaction interface on the CBL TKBD and demonstrate that SLAP/SLAP2 adaptor protein binding to this site is an additional mechanism to regulate CBL ubiquitin ligase activity. Furthermore, the presence of SH2 and SH3 domains as well as a myristoylation modification in SLAP/SLAP2 support a model in which SLAP/SLAP2 binding regulates multiple context specific aspects of CBL function.

bioRxiv preprint doi: https://doi.org/10.1101/2020.06.18.159806; this version posted June 18, 2020. The copyright holder for this preprint (which was not certified by peer review) is the author/funder. All rights reserved. No reuse allowed without permission.

Methods

Cloning, strains, protein overexpression and purification

Residues 28-259 of mouse SLAP2, 29-261 of human SLAP2, or 19-254 of mouse SLAP were cloned in frame into a modified pET32a (pET32a-mod) vector (with a TEV cleavage site downstream of the His tag and 17 residues upstream of the thrombin cleavage site; gift from Gil Prive lab, UHN) with BamHI/BglII and XhoI sites, to express thioredoxin (Trx)-His(6)-mSLAP2, -hSLAP2, and -mSLAP. Using standard QuikChange methods, 19 residues downstream of the TEV cleavage site were deleted from Trx-His(6)-hSLAP2, thus abolishing the thrombin cleavage site and placing the TEV cleavage site in closer proximity to the protein N-terminus, to generate Trx-His(6)-Δlinker-hSLAP2. Trx-His(6)-hSLAP2, Trx-His(6)-Δlinker-hSLAP2, and Trx-His(6)-mSLAP were cloned in frame into multiple cloning site (MCS) 1 of pETDuet-1 (Novagen), with CBL (47-357) cloned in frame into MCS2 of the same pETDuet-1 vector, for co-expression of SLAP2 or SLAP and CBL (Duet-His-hSLAP2-CBL, Duet-His-Δlinker-hSLAP2-CBL, and Duet-His-mSLAP-CBL). Deletion of residues 198-229 and 255-261 from SLAP2 in Duet-His-hSLAP2-CBL and point mutation of residues within Duet-His-Δlinker-hSLAP2-CBL were generated by standard QuikChange site-directed mutagenesis methods. Residues 25-357 and 2-436 of CBL were cloned in frame into pGEX4T-1 to express glutathione-S-transferase (GST)-CBL and GST-CBL TKBD-LHR-RING. Point mutations were generated in Trx-His(6)-hSLAP2 and GST-CBL TKBD-LHR-RING as above. GST-EphA4 (591-896) plasmid was a gift from Frank Sicheri (Lunenfeld-Tanenbaum Research Institute) [76].

For purification of recombinant SLAP2 for crystallization trials and *in vitro* phosphorylation experiments, Trx-His(6)-mSLAP2 was transformed into *E. coli* BL-21 cells and grown in 8 L Luria Bertani (LB) media supplemented with 50 μg/ml ampicillin (Amp) overnight

bioRxiv preprint doi: https://doi.org/10.1101/2020.06.18.159806; this version posted June 18, 2020. The copyright holder for this preprint (which was not certified by peer review) is the author/funder. All rights reserved. No reuse allowed without permission.

at 16°C (A_{600} = 0.6-0.9 and 0.5 mM isopropyl-β-D-thiogalactopyranoside (IPTG) induction). Cells were collected by centrifugation and cell pellet frozen at -80°C. Cell pellet was thawed and resuspended in ~150 mL high-salt lysis buffer (50 mM HEPES pH 7.5, 0.5 M NaCl, 10% glycerol, 10 mM imidazole, 10 mM β-mercaptoethanol (βME), 10 mM $MgCl_2$, 5 mM $CaCl_2$, cOmplete EDTA-free protease inhibitor cocktail tablets (inhibitor tablets) (Roche Applied Science), benzonase nuclease, 1 mM phenylmethylsulfonyl fluoride (PMSF)) and lysed by three cycles of high pressure homogenization (Emulsiflex) and two cycles of sonication on ice. Following centrifugation, supernatant was mixed with Ni-NTA agarose (Qiagen) for 90 min by gently nutating at 4°C. Resin was washed with 6 x 25 mL of wash buffer (50 mM HEPES pH 7.5, 0.5 M NaCl, 10% glycerol, 20 mM imidazole, 10 mM βME, 10 mM $MgCl_2$, 5 mM $CaCl_2$) and SLAP2 protein eluted with wash buffer containing increasing concentrations of imidazole (75, 150, 225, 300 mM imidazole, 28 mL total elution volume). The Trx-His(6) tag was cleaved by addition of 300 units of thrombin (Sigma T4648) directly to the eluate and the solution dialyzed (Slide-A-Lyzer dialysis cassettes, Thermo Scientific, 3500 MWCO) overnight at room temperature (rt) against 2 L dialysis buffer (25 mM Hepes pH 7.5, 0.4 M NaCl, 4% glycerol, 10 mM imidazole, 5 mM βME, 5 mM $MgCl_2$, 5 mM $CaCl_2$). The solution was removed from the dialysis cassette, centrifuged at 4000 rpm for 7 min to remove precipitate, and PMSF added to the soluble portion to 1 mM. This SLAP2 solution was passed very slowly over the same aliquot of Ni-NTA resin (washed since elution) to remove Trx-His(6), concentrated with a centrifugal filter unit (Amicon Ultra, Millipore), and flash frozen in liquid nitrogen for storage at -80°C.

For purification of recombinant CBL for crystallization trials, GST-CBL was overexpressed and cells harvested as above (except 6.5 hours at 37°C or overnight at 30°C and 1 mM IPTG induction). Cell pellet was resuspended in ~100 mL lysis buffer (50 mM HEPES pH

bioRxiv preprint doi: https://doi.org/10.1101/2020.06.18.159806; this version posted June 18, 2020. The copyright holder for this preprint (which was not certified by peer review) is the author/funder. All rights reserved. No reuse allowed without permission.

7.5, 0.5 M NaCl, 10% glycerol, 10 mM βME, 2 mM $MgSO_4$, inhibitor tablets, benzonase nuclease), and lysed as above. Following centrifugation, supernatant was mixed with Glutathione Sepharose 4B (GE Healthcare) for 90 min by nutating at 4°C. Resin was washed with 6 x 25 mL of wash buffer (50 mM HEPES pH 7.5, 0.5 M NaCl, 10% glycerol, 10 mM βME, 5 mM $CaCl_2$) and 150 units of thrombin (Sigma #T4648) added directly to the resin overnight at rt. CBL protein was eluted by washing resin with elution buffer (25 mM HEPES pH 7.5, 0.4 M NaCl, 5% glycerol, 5 mM βME), concentrated as above, and stored stably at 4°C for weeks.

Approximately 33 mg of CBL or 10 mg of mSLAP2 were loaded individually onto a HiLoad 26/60 Superdex 75 gel filtration column (GE Healthcare Life Sciences) equilibrated with GF buffer (25 mM HEPES pH 7.5, 0.4 M NaCl, 2% glycerol, 5 mM βME) and protein elution detected by monitoring A_{280}. Fractions corresponding to isolated CBL or SLAP2 protein were assessed for purity by 12.5% SDS-PAGE analysis. Purified CBL and SLAP2 protein were mixed in a 1:1 molar ratio, concentrated to 1 mL, and loaded onto the same gel filtration column as above. Fractions corresponding to co-elution of CBL and SLAP2 were assessed for purity by 12.5% SDS-PAGE analysis and concentrated to 11.2 mg/mL. (Concentration was estimated by measuring the absorbance of the protein at 280 nm and calculating its concentration using a combined CBL/SLAP2 molecular extinction coefficient of 94810 M^{-1} cm^{-1} as predicted by ProtParam (http://web.expasy.org; [77])).

For co-purification of CBL and SLAP2/SLAP, Duet-His-hSLAP2-CBL 29-261 Δ198-229 and 29-254 Δ198-229, Duet-His-Δlinker-hSLAP2-CBL WT and point mutants, and Duet-His-mSLAP-CBL WT and point mutants were overexpressed in *E. coli* BL-21 as above or TKB1 competent cells (Stratagene) as per manufacturer's instructions, and cells harvested as above (except 100 mL of LB, overnight at 16-18°C, and 0.35-0.5 mM IPTG induction). Cell pellets

bioRxiv preprint doi: https://doi.org/10.1101/2020.06.18.159806; this version posted June 18, 2020. The copyright holder for this preprint (which was not certified by peer review) is the author/funder. All rights reserved. No reuse allowed without permission.

were resuspended in either high or low salt (as for high salt except 25 mM HEPES pH 7.5, 150 mM NaCl) lysis buffer and purified as above on Ni-NTA agarose (Qiagen) with wash buffer (25 mM HEPES pH 7.5, 150 mM NaCl, 2% glycerol, 20 mM imidazole, 10 mM βME). Bead slurry was mixed with SDS 2X loading buffer (125 mM Tris pH 6.8, 4% SDS, 20% glycerol, 0.715 M βME, bromophenol blue), boiled, and analyzed by 10 or 12.5% SDS-PAGE, stained with Coomassie blue.

For purification of SLAP2, pSLAP2, CBL-TKBD-LHR-RING (CBL) and pCBL for ubiquitination assays, GST-CBL-TKBD-LHR-RING and Trx-His(6)-hSLAP2 WT and point mutants were transformed into *E. coli* BL-21 or TKB1 as above. 100 mL cultures were grown overnight at 18°C (A_{600} = 0.6-0.9 and 0.4 mM IPTG induction), pelleted and stored at -80°C. CBL pellets were resuspended in 3 ml each of NP-40 lysis buffer (50 mM HEPES pH 7.5, 150 mM NaCl, 10% glycerol, 1% NP-40, 10 mM NaF, 1.5 mM $MgCl_2$, 1 mM EDTA pH 8.0, 1 mM Na_3VO_4, and inhibitor tablets) and processed as above. CBL and pCBL were purified using Glutathione Sepharose 4B resin as above, followed by three washes with NP-40 wash buffer (20 mM HEPES pH 7.5, 150 mM NaCl, 5% glycerol, 0.1% NP-40, 5 mM βME, 0.5 PMSF, 0.5 mM Na_3VO_4), three washes with PBS wash buffer (PBS pH 7.4, 5 mM βME, 0.5 mM Na_3VO_4), and incubation with thrombin protease. SLAP2 pellets were resuspended in 3 mL each of lysis buffer (50 mM HEPES pH 7.5, 0.5 M NaCl, 10% glycerol, 1% NP-40, 10 mM imidazole, 10 mM NaF, 5 mM βME, 5 mM caproic acid, 1.5 mM $MgCl_2$, 1 mM Na_3VO_4, benzonase nuclease, and inhibitor tablets) and processed as above. SLAP2 and pSLAP2 were isolated using Ni-NTA agarose resin as above, followed by three washes with 50 mM HEPES pH 7.5, 0.5 M NaCl, 2% glycerol, 20 mM imidazole, 5 mM βME, 0.5 mM Na_3VO_4, three washes with PBS wash buffer,

bioRxiv preprint doi: https://doi.org/10.1101/2020.06.18.159806; this version posted June 18, 2020. The copyright holder for this preprint (which was not certified by peer review) is the author/funder. All rights reserved. No reuse allowed without permission.

and incubation with TEV protease. Protein concentrations were determined through Bradford assays.

For purification of GST-EphA4 for *in vitro* phosphorylation experiments, GST-EphA4 was overexpressed and cells harvested as above (except 2L of LB, overnight at rt, and 0.15 mM IPTG induction). Cell pellets were resuspended in lysis buffer (50 mM HEPES pH 7.5, 0.5 M NaCl, 10% glycerol, 3 mM DTT, 1 mM $MgSO_4$, inhibitor tablets, benzonase nuclease) and prepared as above for GST-CBL. Resin was washed with 4 x 25 mL of PBS, pH 7.4, 3 mM DTT.

Crystallization and structure determination

Co-eluted CBL/SLAP2 (5 mg/mL) was mixed in a hanging drop with equal volume (200 nL) of 0.1 M Hepes pH 7.5, 10% (w/v) PEG8000 at rt using a Mosquito robot (TTP Labtech). Small rod-like crystals were observed after approximately five months. A solution of 50% glycerol was added to the drop prior to harvesting and flash freezing the crystals in liquid nitrogen. Diffraction data was collected at the Advanced Photon Source and processed with Mosflm and QuickScale (Pointless, Aimless/Scala, Ctruncate) software to 2.5 Å [78,79]. Molecular replacement was performed with Phenix software (Phaser_MR) [80] using CBL TKBD (PDB id: 1B47) as a model. Anisotropic scaling of the data (services.mbi.ucla.edu/anisoscale) showed strong anisotropy (25.99 $Å^2$) and determined limits of 2.5, 2.8, 2.5 Å. After multiple iterative cycles of model building in Coot and refinement with Phenix_refine [80,81], the Rfree was 33.0%. A Feature Enhanced Map (FEM) was calculated using Phenix software and polyGlycine chains placed in the unassigned density using the "Find Helices and Strands" feature in Phenix, the new FEM, and the improved model. Poly-glycines were manually converted to poly-alanines, and then to mSLAP2 residues ^{240}GLRESLSSYISLAEDP^{255} in both chains of unassigned density.

bioRxiv preprint doi: https://doi.org/10.1101/2020.06.18.159806; this version posted June 18, 2020. The copyright holder for this preprint (which was not certified by peer review) is the author/funder. All rights reserved. No reuse allowed without permission.

Real space refinement in Coot placed the SLAP2 residues perfectly within the previously unassigned density, and refinement in Phenix reduced the Rfree to 31.2%. Using the FEM, residues ^{237}LSE^{239} were assigned, as well as water molecules in the next round of refinement, reducing Rfree to 30.4%. Final rounds of refinement reduced Rfree to 29.3% (Rfactor 24.9%). Symmetry related molecules, distances, superpositions, and root mean square deviations were calculated in Coot [81]. Accessible surface area was calculated with Areaimol from the CCP4 program suite [78]. Coordinates and structure factors were deposited in the Protein Data Bank with accession number 6XAR.

In vitro phosphorylation and detection by mass spectrometry

Purified mSLAP2 was incubated with GST-EphA4, 50 mM Hepes pH 7.5, 20 mM $MgCl_2$, 5 mM adenosine triphosphate (ATP), 5 mM DTT, and 1 mM Na_3VO_3 overnight at rt. Reaction was boiled with SDS 2X loading buffer, loaded on 12.5% SDS-PAGE gel, and transferred to polyvinylidene difluoride (PVDF) membrane. PVDF membrane was immunoblotted with anti-pTyr antibody 4G10 (Upstate Biotechnology, Inc.) as per manufacturer's protocol. A second kinase reaction was boiled with SDS 2X loading buffer and run in multiple lanes of a 15% SDS-PAGE gel. The gel was stained with Coomassie and the upper band observed in the presence of EphA4 excised from the gel. Gel bands were treated and digested with either trypsin or GluC protease as per SPARC BioCentre's in-gel digestion protocol (https://lab.research.sickkids.ca/sparc-molecular-analysis/services/mass-spectrometry/mass-spectrometry-sample-protocols/). Digested peptides were subjected to LC-MS/MS at SPARC BioCentre (The Hospital for Sick Children) (60 min gradient, Thermo LTQ Orbitrap) and the raw data searched with PEAKS software against the mouse proteome, with

bioRxiv preprint doi: https://doi.org/10.1101/2020.06.18.159806; this version posted June 18, 2020. The copyright holder for this preprint (which was not certified by peer review) is the author/funder. All rights reserved. No reuse allowed without permission.

carbamidomethylation as a fixed modification and deamidation (NQ), oxidation (M), and phosphorylation (STY) as variable modifications.

In vitro autoubiquitination assays

In vitro ubiquitination reactions were prepared with 20 pmol of CBL or pCBL and 60 pmol of hSLAP2 or phosphorylated hSLAP2 (pSLAP2) for both WT and mutants. Reagents were thawed and reactions prepared on ice. CBL and SLAP2 were mixed in PBS (with 5 mM βME, 5 mM caproic acid, 0.5 mM PMSF, and 0.5 mM Na_3VO_4) at rt for 5-10 min before addition of master mix (42 pmol E1 (UBE1, Boston Biochem or Ubiquitin-Proteasome Biotechnologies), 0.1 μmol E2 (UbcH5b/UBE2D2, Boston Biochem #E2-622), 1 mmol ATP, and 11.6 μmol ubiquitin (Boston Biochem #U-100H) in reaction buffer (0.2 M Tris pH 7.5, 10 mM $MgCl_2$, 2 mM DTT). Reactions were incubated at 30°C shaking at 500-700 rpm for 60-110 minutes and terminated by addition of SDS 2X loading buffer and boiling for 5-10 minutes. Equal volumes of each reaction were loaded on 12.5% SDS-PAGE gel, transferred to PVDF membrane, and immunoblotted for ubiquitin as per standard protocols (anti-ubiquitin antibody P4G7, BioLegend #838701, 1:1000; anti-mouse IgG HRP-linked antibody, Cell Signaling Technology #7076, 1:10000; Western Lightning Plus ECL, Perkin Elmer).

Ubiquitination reactions were set up as above (25 μL total volume) in triplicate and diluted with reaction buffer after completion (1:40 for pCBL, 1:15 for all other reactions). Each reaction triplicate was added in triplicate to individual wells of a 384-well E3LITE Customizable Ubiquitin Ligase Kit (Life Sensors) plate, prewashed three times with PBS, and incubated for 60 minutes at rt on a rotating platform to capture ubiquitinated proteins. Wells were washed three

bioRxiv preprint doi: https://doi.org/10.1101/2020.06.18.159806; this version posted June 18, 2020. The copyright holder for this preprint (which was not certified by peer review) is the author/funder. All rights reserved. No reuse allowed without permission.

times with PBS plus 0.1% Tween (PBS-T) and 25 uL of detection solution 1 (1:1000 dilution in PBS-T + 5% BSA) added to each well. After 50 min incubation, the wells were washed three times with PBS-T, 25 µL of streptavidin peroxidase polymer ultrasensitive antibody (Sigma #S2438, 1:10000 dilution in PBS-T, 5% BSA) added to each well, and the plate incubated for 50 min. Wells were washed four times with PBS-T and 25 µL of prepared Immobilon Western Chemiluminescent HRP Substrate (Millipore #P90719) added to each well immediately prior to the plate being read on a Synergy Neo2 Plate Reader (BioTek Instruments). The average luminescent signal for each condition was divided by that of CBL WT to determine fold change over CBL. Standard deviation of the reaction averages was calculated and used as a measure of error. Each reaction set was analyzed at least twice with fresh protein purifications.

LC-MS analysis of ubiquitination reactions

Relative ubiquitin linkages levels were measured by LC-MS via monitoring of diglycine(GG)-modified ubiquitin "linkage reporter" peptides [57]. *In vitro* autoubiquitination reactions were prepared as above, lyophilized, re-suspended in 9 M urea, 100 mM NH_4HCO_3, 5 mM DTT, and incubated for 20 min at 60°C. Samples were cooled to rt, treated with 10 mM iodoacetamide for 30 min at rt in the dark, and diluted with 50 mM NH_4HCO_3 to a final urea concentration of ~2M. Sequencing-grade, TPCK-treated, modified trypsin (Promega) was added (1 µg) for 16 hrs at 37°C. The resulting peptide samples were desalted using C18 tips and lyophilized. Peptides were re-suspended in 0.1% HCOOH and analyzed by LC-MS/MS. LC was conducted using a C18 pre-column (Acclaim PepMap 100, 2 cm x 75 µm ID, Thermo Scientific) and a C18 analytical column (Acclaim PepMap RSLC, 50 cm x 75 µm ID, Thermo Scientific) over a 120 min reversed-phase gradient (0-40% ACN in 0.1% HCOOH) at 225 nl/min on an

bioRxiv preprint doi: https://doi.org/10.1101/2020.06.18.159806; this version posted June 18, 2020. The copyright holder for this preprint (which was not certified by peer review) is the author/funder. All rights reserved. No reuse allowed without permission.

EASY-nLC1200 pump (Proxeon) in-line with a Q-Exactive HF mass spectrometer (Thermo Scientific). A MS scan was performed with a resolution of 60,000 followed by up to 20 MS/MS scans (minimum ion count of 1000 for activation) using higher energy collision induced dissociation (HCD) fragmentation. Dynamic exclusion was set for 5 seconds (10 ppm; exclusion list size = 500). For peptide and protein identification, Thermo .RAW files were converted to .mzML format using ProteoWizard (v3.0.10800; [82]), then searched using X!Tandem (X!TANDEM Jackhammer TPP v2013.06.15.1; [83]) and Comet (v2014.02 rev.2; [84]) against the human RefSeq v45 database (containing 36113 entries). Search parameters specified a parent ion mass tolerance of 10 ppm and an MS/MS fragment ion tolerance of 0.4 Da, with up to two missed cleavages allowed for trypsin (excluding K/RP). Variable modifications of 0.984013 on N/Q, 15.99491 on M, 114.04293 on K, 79.96633 Y/S/T and 57.021459 on C were allowed. Data were filtered through the TPP (v4.7 POLAR VORTEX rev 1) with general parameters set as –p0.05 -x20 –PPM. For label-free MS1-level quantification, raw files were analyzed using MaxQuant (v1.6; [85]).

Ubiquitination and substrate binding in cells

COS-7 cells were serum starved for 24 hours (~80% confluent), followed by a 15 minute stimulation with 100 ng/mL EGF. Cells were lysed in 200 µL PLC lysis buffer/plate (50 mM HEPES pH 7.5, 150 mM NaCl, 1.5 mM $MgCl_2$, 1 mM EGTA pH 8.0, 10% glycerol, 1% Triton X-100, supplemented with 10 mM NaF, Na_3VO_4, cOmplete EDTA-protease inhibitor tablet (Roche)) and protein concentration determined by Bradford assay. Lysate (500 µg) was incubated for 2 hours at 4°C with the equivalent of 30 µg GST-CBL-TKBD-LHR-RING WT or

bioRxiv preprint doi: https://doi.org/10.1101/2020.06.18.159806; this version posted June 18, 2020. The copyright holder for this preprint (which was not certified by peer review) is the author/funder. All rights reserved. No reuse allowed without permission.

mutants captured on Glutathione Sepharose 4B as above. Samples were prepared for SDS-PAGE and immunoblot as described above, with anti-EGFR antibody (D38B1; Cell Signaling Tech).

HEK 293T cells were transfected using Lipofectamine 2000 (ThermoFisher), as per manufacturer's instructions and standard procedures, with 3 μg HA-tagged full length CBL (in pCDEF3), 1 μg FLAG-tagged EGFR (in pcDNA 3.1), and/or 3 μg His-Ubiquitin (octameric ubiquitin construct with N-terminal His_6 tag for each), as indicated. Promoter matched backbone DNA was used where necessary to give 7 μg of DNA per plate for all conditions. After 24 hours, cells were harvested in cold PBS, pelleted by centrifugation, lysed in cold PLC lysis buffer, and protein concentration measured by Bradford assay. For lysate immunoblots, 50 μg samples were prepared in 2X SDS loading buffer and boiled for 10 min. For immunoprecipitation, 1 mg of lysate was incubated with pre-washed anti-FLAG M2 affinity gel (Sigma-Aldrich, #A2220) for 2 hours at 4°C with gentle nutation. Resin was pelleted at 5000 rcf for 30 seconds at 4°C and washed three times with lysis buffer. After the last wash, resin was mixed with 70 μL of 2X SDS loading buffer and boiled for 10 minutes. For immunoblotting, immunoprecipitation samples were divided between two gels. Lysate and immunoprecipitation samples were resolved by 8% SDS-PAGE and immunoblotted using standard protocols as described above. Where indicated, the following primary antibodies were used: 1 μg/mL anti-FLAG M2 (Sigma-Aldrich #F1804), 0.2 μg/mL anti-HA F-7 (Santa Cruz Biotechnology #sc7392), 0.5 μg/mL anti-His_6 (Roche #11 922 416 001). Total protein on lysate membranes was stained with 50% methanol with 0.1% Coomassie Brilliant Blue R-250 dye, and destained in 50% methanol, 10% acetic acid. The His-Ub, FLAG (EGFR) signals were quantified for the FLAG immunoprecipitation using Image Lab (BioRad Laboritories, version 6.0 build 26). Lanes and bands were manually defined using the volume tool. Background adjusted volume measurements were obtained for the FLAG and His

bioRxiv preprint doi: https://doi.org/10.1101/2020.06.18.159806; this version posted June 18, 2020. The copyright holder for this preprint (which was not certified by peer review) is the author/funder. All rights reserved. No reuse allowed without permission.

signals for three replicates of the FLAG immunoprecipitation (IP) experiment in conditions where FLAG-EGFR was transfected. His-Ub signals were normalized to the corresponding FLAG signal for each replicate. The average normalized intensities were plotted, showing the corresponding individual values as points, and error bars representing the standard deviation.

bioRxiv preprint doi: https://doi.org/10.1101/2020.06.18.159806; this version posted June 18, 2020. The copyright holder for this preprint (which was not certified by peer review) is the author/funder. All rights reserved. No reuse allowed without permission.

Acknowledgements: The authors thank Savar Kaul, Julia Manalil, Alissa Visram, Mackenzie Kinney, Donna Berry, Jessica Lapierre and Andrew Bondoc for technical assistance, Elton Zeqiraj for diffraction data collection, and Frank Sicheri for access to crystallization resources and diffraction data collection. This work was supported with funds from the Cancer Research Society, Garron Family Cancer Centre, and the Canadian Institutes of Health Research FRN166034(to CJM). LWG was support by fellowships from CIHR and ABTA, AT is funded by an Ontario Graduate Scholarship and RESTRACOMP.

Author Contributions: LEW-G, AT and CS performed experiments and wrote the manuscript; JSG performed experiments; MM supervised and BR supervised JSG. CJM supervised LEW-G, CS, AT and wrote the manuscript.

Competing Interest Statement: The authors declare no conflict of interest.

bioRxiv preprint doi: https://doi.org/10.1101/2020.06.18.159806; this version posted June 18, 2020. The copyright holder for this preprint (which was not certified by peer review) is the author/funder. All rights reserved. No reuse allowed without permission.

References:

1 Hershko, A. & Ciechanover, A. The ubiquitin system. *Annu Rev Biochem* **67**, 425-479 (1998).

2 Kerscher, O., Felberbaum, R. & Hochstrasser, M. Modification of proteins by ubiquitin and ubiquitin-like proteins. *Annu Rev Cell Dev Biol* **22**, 159-180, doi:10.1146/annurev.cellbio.22.010605.093503 (2006).

3 Deshaies, R. J. & Joazeiro, C. A. RING domain E3 ubiquitin ligases. *Annu Rev Biochem* **78**, 399-434, doi:10.1146/annurev.biochem.78.101807.093809 (2009).

4 Rotin, D. & Kumar, S. Physiological functions of the HECT family of ubiquitin ligases. *Nat Rev Mol Cell Biol* **10**, 398-409, doi:10.1038/nrm2690 (2009).

5 Thien, C. B. & Langdon, W. Y. Negative regulation of PTK signalling by Cbl proteins. *Growth Factors* **23**, 161-167 (2005).

6 Marmor, M. D. & Yarden, Y. Role of protein ubiquitylation in regulating endocytosis of receptor tyrosine kinases. *Oncogene* **23**, 2057-2070 (2004).

7 Mohapatra, B. *et al.* Protein tyrosine kinase regulation by ubiquitination: critical roles of Cbl-family ubiquitin ligases. *Biochim Biophys Acta* **1833**, 122-139, doi:10.1016/j.bbamcr.2012.10.010 (2013).

8 Clague, M. J., Liu, H. & Urbe, S. Governance of endocytic trafficking and signaling by reversible ubiquitylation. *Dev Cell* **23**, 457-467, doi:10.1016/j.devcel.2012.08.011 (2012).

9 Joazeiro, C. A. *et al.* The tyrosine kinase negative regulator c-Cbl as a RING-type, E2-dependent ubiquitin-protein ligase. *Science* **286**, 309-312 (1999).

10 Acconcia, F., Sigismund, S. & Polo, S. Ubiquitin in trafficking: the network at work. *Exp Cell Res* **315**, 1610-1618, doi:10.1016/j.yexcr.2008.10.014 (2009).

11 Urbe, S. Ubiquitin and endocytic protein sorting. *Essays Biochem* **41**, 81-98 (2005).

12 Thien, C. B., Bowtell, D. D. & Langdon, W. Y. Perturbed regulation of ZAP-70 and sustained tyrosine phosphorylation of LAT and SLP-76 in c-Cbl-deficient thymocytes. *J Immunol* **162**, 7133-7139 (1999).

13 Yokouchi, M. *et al.* Src-catalyzed phosphorylation of c-Cbl leads to the interdependent ubiquitination of both proteins. *J Biol Chem* **276**, 35185-35193 (2001).

14 Andoniou, C. E. *et al.* The Cbl proto-oncogene product negatively regulates the Src-family tyrosine kinase Fyn by enhancing its degradation. *Mol Cell Biol* **20**, 851-867 (2000).

15 Meng, W., Sawasdikosol, S., Burakoff, S. J. & Eck, M. J. Structure of the amino-terminal domain of Cbl complexed to its binding site on ZAP-70 kinase. *Nature* **398**, 84-90 (1999).

16 Levkowitz, G. *et al.* Ubiquitin ligase activity and tyrosine phosphorylation underlie suppression of growth factor signaling by c-Cbl/Sli-1. *Mol Cell* **4**, 1029-1040 (1999).

17 Ryan, P. E., Sivadasan-Nair, N., Nau, M. M., Nicholas, S. & Lipkowitz, S. The N terminus of Cbl-c regulates ubiquitin ligase activity by modulating affinity for the ubiquitin-conjugating enzyme. *J Biol Chem* **285**, 23687-23698 (2010).

bioRxiv preprint doi: https://doi.org/10.1101/2020.06.18.159806; this version posted June 18, 2020. The copyright holder for this preprint (which was not certified by peer review) is the author/funder. All rights reserved. No reuse allowed without permission.

18 Liu, J., Kimura, A., Baumann, C. A. & Saltiel, A. R. APS facilitates c-Cbl tyrosine phosphorylation and GLUT4 translocation in response to insulin in 3T3-L1 adipocytes. *Mol Cell Biol* **22**, 3599-3609 (2002).

19 Kassenbrock, C. K. & Anderson, S. M. Regulation of ubiquitin protein ligase activity in c-Cbl by phosphorylation-induced conformational change and constitutive activation by tyrosine to glutamate point mutations. *J Biol Chem* **279**, 28017-28027 (2004).

20 Zheng, N., Wang, P., Jeffrey, P. D. & Pavletich, N. P. Structure of a c-Cbl-UbcH7 complex: RING domain function in ubiquitin-protein ligases. *Cell* **102**, 533-539 (2000).

21 Dou, H. *et al.* Structural basis for autoinhibition and phosphorylation-dependent activation of c-Cbl. *Nat Struct Mol Biol* **19**, 184-192 (2012).

22 Dou, H., Buetow, L., Sibbet, G. J., Cameron, K. & Huang, D. T. Essentiality of a non-RING element in priming donor ubiquitin for catalysis by a monomeric E3. *Nat Struct Mol Biol* **20**, 982-986, doi:10.1038/nsmb.2621 (2013).

23 Kales, S. C., Ryan, P. E., Nau, M. M. & Lipkowitz, S. Cbl and human myeloid neoplasms: the Cbl oncogene comes of age. *Cancer Res* **70**, 4789-4794 (2010).

24 Ogawa, S. *et al.* Deregulated intracellular signaling by mutated c-CBL in myeloid neoplasms. *Clin Cancer Res* **16**, 3825-3831 (2010).

25 Grand, F. H. *et al.* Frequent CBL mutations associated with 11q acquired uniparental disomy in myeloproliferative neoplasms. *Blood* **113**, 6182-6192 (2009).

26 Loh, M. L. *et al.* Mutations in CBL occur frequently in juvenile myelomonocytic leukemia. *Blood* **114**, 1859-1863, doi:10.1182/blood-2009-01-198416 (2009).

27 Makishima, H. *et al.* Mutations of e3 ubiquitin ligase cbl family members constitute a novel common pathogenic lesion in myeloid malignancies. *J Clin Oncol* **27**, 6109-6116 (2009).

28 Swaminathan, G. & Tsygankov, A. Y. The Cbl family proteins: ring leaders in regulation of cell signaling. *J Cell Physiol* **209**, 21-43 (2006).

29 Javadi, M., Richmond, T. D., Huang, K. & Barber, D. L. CBL linker region and RING finger mutations lead to enhanced granulocyte-macrophage colony-stimulating factor (GM-CSF) signaling via elevated levels of JAK2 and LYN. *J Biol Chem* **288**, 19459-19470, doi:10.1074/jbc.M113.475087 (2013).

30 Nadeau, S. A. *et al.* Structural Determinants of the Gain-of-Function Phenotype of Human Leukemia-associated Mutant CBL Oncogene. *J Biol Chem* **292**, 3666-3682, doi:10.1074/jbc.M116.772723 (2017).

31 Sosinowski, T., Pandey, A., Dixit, V. M. & Weiss, A. Src-like adaptor protein (SLAP) is a negative regulator of T cell receptor signaling. *J Exp Med* **191**, 463-474 (2000).

32 Loreto, M. P. & McGlade, C. J. Cloning and characterization of human Src-like adaptor protein 2 and a novel splice isoform, SLAP-2-v. *Oncogene* **22**, 266-273 (2003).

33 Loreto, M. P., Berry, D. M. & McGlade, C. J. Functional cooperation between c-Cbl and Src-like adaptor protein 2 in the negative regulation of T-cell receptor signaling. *Mol Cell Biol* **22**, 4241-4255 (2002).

34 Sosinowski, T., Killeen, N. & Weiss, A. The Src-like adaptor protein downregulates the T cell receptor on CD4+CD8+ thymocytes and regulates positive selection. *Immunity* **15**, 457-466 (2001).

35 Myers, M. D. *et al.* Src-like adaptor protein regulates TCR expression on thymocytes by linking the ubiquitin ligase c-Cbl to the TCR complex. *Nat Immunol* **7**, 57-66 (2006).

bioRxiv preprint doi: https://doi.org/10.1101/2020.06.18.159806; this version posted June 18, 2020. The copyright holder for this preprint (which was not certified by peer review) is the author/funder. All rights reserved. No reuse allowed without permission.

36 Dragone, L. L. *et al.* Src-like adaptor protein (SLAP) regulates B cell receptor levels in a c-Cbl-dependent manner. *Proc Natl Acad Sci U S A* **103**, 18202-18207 (2006).
37 Dragone, L. L., Shaw, L. A., Myers, M. D. & Weiss, A. SLAP, a regulator of immunoreceptor ubiquitination, signaling, and trafficking. *Immunol Rev* **232**, 218-228 (2009).
38 Naramura, M., Kole, H. K., Hu, R. J. & Gu, H. Altered thymic positive selection and intracellular signals in Cbl-deficient mice. *Proc Natl Acad Sci U S A* **95**, 15547-15552 (1998).
39 Lebigot, I. *et al.* Up-regulation of SLAP in FLI-1-transformed erythroblasts interferes with EpoR signaling. *Blood* **102**, 4555-4562 (2003).
40 Liontos, L. M. *et al.* The Src-like adaptor protein regulates GM-CSFR signaling and monocytic dendritic cell maturation. *J Immunol* **186**, 1923-1933 (2011).
41 Cherpokova, D. *et al.* SLAP/SLAP2 prevent excessive platelet (hem)ITAM signaling in thrombosis and ischemic stroke in mice. *Blood* **125**, 185-194, doi:10.1182/blood-2014-06-580597 (2015).
42 Pakuts, B., Debonneville, C., Liontos, L. M., Loreto, M. P. & McGlade, C. J. The Src-like adaptor protein 2 regulates colony-stimulating factor-1 receptor signaling and down-regulation. *J Biol Chem* **282**, 17953-17963 (2007).
43 Wybenga-Groot, L. E. & McGlade, C. J. RTK SLAP DOWN: The emerging role of Src-like adaptor protein as a key player in receptor tyrosine kinase signaling. *Cell Signal* **27**, 267-274, doi:10.1016/j.cellsig.2014.11.010 (2015).
44 Kazi, J. U., Agarwal, S., Sun, J., Bracco, E. & Ronnstrand, L. Src-like-adaptor protein (SLAP) differentially regulates normal and oncogenic c-Kit signaling. *J Cell Sci* **127**, 653-662, doi:10.1242/jcs.140590 (2014).
45 Kazi, J. U. & Ronnstrand, L. Src-Like adaptor protein (SLAP) binds to the receptor tyrosine kinase Flt3 and modulates receptor stability and downstream signaling. *PLoS One* **7**, e53509, doi:10.1371/journal.pone.0053509 (2012).
46 Roche, S. *et al.* Src-like adaptor protein (Slap) is a negative regulator of mitogenesis. *Curr Biol* **8**, 975-978 (1998).
47 Sirvent, A., Leroy, C., Boureux, A., Simon, V. & Roche, S. The Src-like adaptor protein regulates PDGF-induced actin dorsal ruffles in a c-Cbl-dependent manner. *Oncogene* **27**, 3494-3500 (2008).
48 Naudin, C. *et al.* SLAP displays tumour suppressor functions in colorectal cancer via destabilization of the SRC substrate EPHA2. *Nat Commun* **5**, 3159, doi:10.1038/ncomms4159 (2014).
49 Pandey, A., Duan, H. & Dixit, V. M. Characterization of a novel Src-like adapter protein that associates with the Eck receptor tyrosine kinase. *J Biol Chem* **270**, 19201-19204 (1995).
50 Tang, J., Sawasdikosol, S., Chang, J. H. & Burakoff, S. J. SLAP, a dimeric adapter protein, plays a functional role in T cell receptor signaling. *Proc Natl Acad Sci U S A* **96**, 9775-9780 (1999).
51 Wybenga-Groot, L. E. & McGlade, C. J. Crystal structure of Src-like adaptor protein 2 reveals close association of SH3 and SH2 domains through beta-sheet formation. *Cell Signal* **25**, 2702-2708, doi:10.1016/j.cellsig.2013.08.040 (2013).
52 Pawson, T. Dynamic control of signaling by modular adaptor proteins. *Curr Opin Cell Biol* **19**, 112-116, doi:10.1016/j.ceb.2007.02.013 (2007).

bioRxiv preprint doi: https://doi.org/10.1101/2020.06.18.159806; this version posted June 18, 2020. The copyright holder for this preprint (which was not certified by peer review) is the author/funder. All rights reserved. No reuse allowed without permission.

53 Holland, S. J. *et al.* Functional cloning of Src-like adapter protein-2 (SLAP-2), a novel inhibitor of antigen receptor signaling. *J Exp Med* **194**, 1263-1276 (2001).
54 Abe, A. *et al.* Establishment of a stroma-dependent human acute myelomonocytic leukemia cell line, NAMO-2, with FLT3 tandem duplication. *Int J Hematol* **84**, 328-336 (2006).
55 Manes, G. A. *et al.* A potential role for the Src-like adapter protein SLAP-2 in signaling by the colony stimulating factor-1 receptor. *Febs J* **273**, 1791-1804 (2006).
56 Drozdetskiy, A., Cole, C., Procter, J. & Barton, G. J. JPred4: a protein secondary structure prediction server. *Nucleic Acids Res* **43**, W389-394, doi:10.1093/nar/gkv332 (2015).
57 Hong, J. H., Ng, D., Srikumar, T. & Raught, B. The use of ubiquitin lysine mutants to characterize E2-E3 linkage specificity: Mass spectrometry offers a cautionary "tail". *Proteomics* **15**, 2910-2915, doi:10.1002/pmic.201500058 (2015).
58 Fong, C. W. *et al.* Tyrosine phosphorylation of Sprouty2 enhances its interaction with c-Cbl and is crucial for its function. *J Biol Chem* **278**, 33456-33464, doi:10.1074/jbc.M301317200 (2003).
59 Wong, E. S., Lim, J., Low, B. C., Chen, Q. & Guy, G. R. Evidence for direct interaction between Sprouty and Cbl. *J Biol Chem* **276**, 5866-5875, doi:10.1074/jbc.M006945200 (2001).
60 Hu, J. & Hubbard, S. R. Structural characterization of a novel Cbl phosphotyrosine recognition motif in the APS family of adapter proteins. *J Biol Chem* **280**, 18943-18949, doi:10.1074/jbc.M414157200 (2005).
61 Dunker, A. K. *et al.* The unfoldomics decade: an update on intrinsically disordered proteins. *BMC Genomics* **9 Suppl 2**, S1, doi:10.1186/1471-2164-9-S2-S1 (2008).
62 Iakoucheva, L. M. *et al.* The importance of intrinsic disorder for protein phosphorylation. *Nucleic Acids Res* **32**, 1037-1049, doi:10.1093/nar/gkh253 (2004).
63 Nau, M. M. & Lipkowitz, S. Comparative genomic organization of the cbl genes. *Gene* **308**, 103-113, doi:10.1016/s0378-1119(03)00471-2 (2003).
64 Keane, M. M., Rivero-Lezcano, O. M., Mitchell, J. A., Robbins, K. C. & Lipkowitz, S. Cloning and characterization of cbl-b: a SH3 binding protein with homology to the c-cbl proto-oncogene. *Oncogene* **10**, 2367-2377 (1995).
65 Kobashigawa, Y. *et al.* Autoinhibition and phosphorylation-induced activation mechanisms of human cancer and autoimmune disease-related E3 protein Cbl-b. *Proc Natl Acad Sci U S A* **108**, 20579-20584, doi:10.1073/pnas.1110712108 (2011).
66 Sharma, N. *et al.* SLAP Is a Negative Regulator of FcepsilonRI Receptor-Mediated Signaling and Allergic Response. *Front Immunol* **10**, 1020, doi:10.3389/fimmu.2019.01020 (2019).
67 Ryan, P. E. *et al.* Cbl-c ubiquitin ligase activity is increased via the interaction of its RING finger domain with a LIM domain of the paxillin homolog, Hic 5. *PLoS One* **7**, e49428, doi:10.1371/journal.pone.0049428 (2012).
68 Ogunjimi, A. A. *et al.* Regulation of Smurf2 ubiquitin ligase activity by anchoring the E2 to the HECT domain. *Mol Cell* **19**, 297-308, doi:10.1016/j.molcel.2005.06.028 (2005).
69 Wiesner, S. *et al.* Autoinhibition of the HECT-type ubiquitin ligase Smurf2 through its C2 domain. *Cell* **130**, 651-662, doi:10.1016/j.cell.2007.06.050 (2007).
70 Buetow, L. & Huang, D. T. Structural insights into the catalysis and regulation of E3 ubiquitin ligases. *Nat Rev Mol Cell Biol* **17**, 626-642, doi:10.1038/nrm.2016.91 (2016).

bioRxiv preprint doi: https://doi.org/10.1101/2020.06.18.159806; this version posted June 18, 2020. The copyright holder for this preprint (which was not certified by peer review) is the author/funder. All rights reserved. No reuse allowed without permission.

71 Kales, S. C., Ryan, P. E. & Lipkowitz, S. Cbl exposes its RING finger. *Nat Struct Mol Biol* **19**, 131-133, doi:10.1038/nsmb.2241 (2012).
72 Dragone, L. L., Myers, M. D., White, C., Sosinowski, T. & Weiss, A. SRC-like adaptor protein regulates B cell development and function. *J Immunol* **176**, 335-345 (2006).
73 Myers, M. D., Dragone, L. L. & Weiss, A. Src-like adaptor protein down-regulates T cell receptor (TCR)-CD3 expression by targeting TCRzeta for degradation. *J Cell Biol* **170**, 285-294 (2005).
74 Wang, H. *et al.* Tonic ubiquitylation controls T-cell receptor:CD3 complex expression during T-cell development. *EMBO J* **29**, 1285-1298, doi:10.1038/emboj.2010.10 (2010).
75 Buetow, L. *et al.* Casitas B-lineage lymphoma linker helix mutations found in myeloproliferative neoplasms affect conformation. *BMC Biol* **14**, 76, doi:10.1186/s12915-016-0298-6 (2016).
76 Wybenga-Groot, L. E. *et al.* Structural basis for autoinhibition of the Ephb2 receptor tyrosine kinase by the unphosphorylated juxtamembrane region. *Cell* **106**, 745-757 (2001).
77 Gasteiger, E. *et al.* ExPASy: The proteomics server for in-depth protein knowledge and analysis. *Nucleic Acids Res* **31**, 3784-3788, doi:10.1093/nar/gkg563 (2003).
78 Winn, M. D. *et al.* Overview of the CCP4 suite and current developments. *Acta Crystallogr D Biol Crystallogr* **67**, 235-242, doi:10.1107/S0907444910045749 (2011).
79 Evans, P. R. An introduction to data reduction: space-group determination, scaling and intensity statistics. *Acta Crystallogr D Biol Crystallogr* **67**, 282-292, doi:10.1107/S090744491003982X (2011).
80 Adams, P. D. *et al.* PHENIX: a comprehensive Python-based system for macromolecular structure solution. *Acta Crystallogr D Biol Crystallogr* **66**, 213-221, doi:10.1107/S0907444909052925 (2010).
81 Emsley, P. & Cowtan, K. Coot: model-building tools for molecular graphics. *Acta Crystallogr D Biol Crystallogr* **60**, 2126-2132, doi:10.1107/S0907444904019158 (2004).
82 Kessner, D., Chambers, M., Burke, R., Agus, D. & Mallick, P. ProteoWizard: open source software for rapid proteomics tools development. *Bioinformatics* **24**, 2534-2536, doi:10.1093/bioinformatics/btn323 (2008).
83 Craig, R. & Beavis, R. C. TANDEM: matching proteins with tandem mass spectra. *Bioinformatics* **20**, 1466-1467, doi:10.1093/bioinformatics/bth092 (2004).
84 Eng, J. K., Jahan, T. A. & Hoopmann, M. R. Comet: an open-source MS/MS sequence database search tool. *Proteomics* **13**, 22-24, doi:10.1002/pmic.201200439 (2013).
85 Cox, J. & Mann, M. MaxQuant enables high peptide identification rates, individualized p.p.b.-range mass accuracies and proteome-wide protein quantification. *Nat Biotechnol* **26**, 1367-1372, doi:10.1038/nbt.1511 (2008).

bioRxiv preprint doi: https://doi.org/10.1101/2020.06.18.159806; this version posted June 18, 2020. The copyright holder for this preprint (which was not certified by peer review) is the author/funder. All rights reserved. No reuse allowed without permission.

Table 1 Data collection and refinement statistics

Data collection	
Space group	$P2_1$
Cell dimensions	
a, *b*, *c* (Å)	62.7, 87.0, 65.3
a, *b*, *g* (°)	90, 112.3, 90
Resolution (Å)	45.3-2.5
R_{merge}	8.0 (60.1)*
I/sI	8.3 (1.5)
Completeness (%)	90.5 (57.8)
Redundancy	2.9 (2.0)
Refinement	
Resolution (Å)	45.3-2.5
No. reflections	18869
R_{work}/R_{free}	24.9/29.3
Number of non-hydrogen atoms	
Macromolecules	4954
Ligands	2
Solvent	47
Average B-factors (Å^2)	48.5
R.m.s deviations	
Bond lengths (Å)	0.002
Bond angles (°)	0.602
Molprobity Statistics	
All-atom clashscore	6.0
Ramachandran	
Favored (%)	93.5
Allowed (%)	99.2

*Highest resolution shell is shown in parenthesis.

bioRxiv preprint doi: https://doi.org/10.1101/2020.06.18.159806; this version posted June 18, 2020. The copyright holder for this preprint (which was not certified by peer review) is the author/funder. All rights reserved. No reuse allowed without permission.

Figure legends:

Figure 1: CBL interacts with C-terminal tail of SLAP2

A) Cartoon of CBL and SLAP2 domains, with arrow indicating interaction between TKBD and SLAP2 C-tail region. B) SDS-PAGE gel stained with Coomassie blue for CBL and SLAP2 proteins co-purified under low salt conditions from Duet-His-Δlinker-hSLAP2-CBL (261), its truncated version (254), Duet-His-hSLAP2-CBL 29-261 Δ198-229, and its truncated version 29-254 Δ198-229. C) Sequence alignment of the C-tail region of SLAP proteins, with residue numbering based on human SLAP2. Conserved Tyr248 is marked with a red box. Secondary structure prediction for mSLAP2 (Jnet pred) and confidence score (Jnet Rel) as calculated by Jnet [56] is shown, with e, -, and h representing β-strand, coil and α-helix, respectively. The secondary structure elements of mSLAP2 as determined by X-ray crystallography are shown in green, with the line and box representing coil and α-helix, respectively.

Figure 2: Crystal structure of CBL and SLAP2

A) Electron density at the site of CBL and SLAP2 interaction is shown in grey, with CBL and SLAP2 atoms shown in stick. Carbon atoms are coloured according to their respective backbones, with CBL monomers in blue and SLAP2 monomers in green. Oxygen and nitrogen atoms are coloured red and blue, respectively. For clarity, portions of CBL in the plane of the page have been removed. B) Ribbon representations of the Cα atoms of the CBL/SLAP2 crystal structure, coloured as in A, with elements of CBL TKBD labelled. Panels are related by a rotation of approximately 90° about the horizontal axis. C) Superposition of the Cα atoms of the 4H bundle and EF-hand of CBL/SLAP2 (PDB id: 6XAR) with those of unliganded (PDB id: 1B47) and liganded CBL TKBD (PDB id: 2Cbl), shown in blue, cyan, and magenta,

bioRxiv preprint doi: https://doi.org/10.1101/2020.06.18.159806; this version posted June 18, 2020. The copyright holder for this preprint (which was not certified by peer review) is the author/funder. All rights reserved. No reuse allowed without permission.

respectively. All ribbon diagrams were prepared with Pymol (The PyMOL Molecular Graphics System, Version 1.5.0.4 Schrödinger, LLC.).

Figure 3: Validation of CBL/SLAP2 interaction by mutagenesis

A) Ribbon representation of the Cα atoms of the CBL/SLAP2 crystal structure, with a pTyr peptide modeled in magenta. Subdomains of CBL TKBD are shown, with the 4H bundle in teal, EF-hand in dark blue, and SH2 domain in light blue. SLAP2 is coloured green. B) As in A, showing the CBL regulatory cleft. C) Magnification of the CBL/SLAP2 interface, coloured as in A, with side chains of CBL, SLAP2 molecule 1, and SLAP2 molecule 2 shown in stick and labelled in teal/dark blue/light blue, black, and green, according to their respective backbones. Oxygen, nitrogen, and sulfur atoms are coloured red, blue, and yellow, respectively. D) SDS-PAGE gel stained with Coomassie blue for CBL and SLAP2 proteins co-purified under high salt (upper panel) and low salt (lower panel) conditions from Duet-His-Δlinker-hSLAP2-CBL and its mutated variants. SLAP2 and CBL mutants are labelled in black and blue, respectively. E) As in D, for SLAP2/SLAP2 interface mutants, co-purified in low salt conditions. F) As in D, for CBL and SLAP proteins co-purified in low salt conditions from Duet-His-mSLAP-CBL and its mutated variants.

Figure 4: Phosphorylation of SLAP2 at tyrosine 248

A) SDS-PAGE gel stained with Coomassie blue for SLAP2 and SLAP2 incubated with EphA4 kinase under phosphorylating conditions (left panel). Immunoblot of SLAP2 +/- EphA4, immunoblotted with anti-pTyr (right panel). B) SDS-PAGE gel as in A, with EphA4 alone also shown. Box indicates upper gel band excised for mass spectrometry analysis. C) Intensity versus

bioRxiv preprint doi: https://doi.org/10.1101/2020.06.18.159806; this version posted June 18, 2020. The copyright holder for this preprint (which was not certified by peer review) is the author/funder. All rights reserved. No reuse allowed without permission.

charge to mass ratio (m/z) plot for SLAP2 C-tail peptides ESLSSY$_{248}$ISLAEDPLDDA (upper panel) and SLSSY$_{248}$ISLAEDPLDDA (lower panel) generated by protease digestion of gel band from B with trypsin and GluC, respectively, followed by LC-MS/MS analysis. D) SDS-PAGE gel stained with Coomassie blue for CBL and SLAP2 WT or Y248F co-purified under low salt conditions from Duet-His-Δlinker-hSLAP2-CBL expressed in normal (BL21) or phosphorylating (TKB1) conditions. E) Ribbon representation of the Cα atoms of the CBL/SLAP2 interface, with CBL shown in blue and SLAP2 in green. Residues of CBL and SLAP2 are shown in stick with carbon atoms coloured according to their respective backbones, and oxygen, nitrogen, sulfur, and phosphorus atoms coloured red, blue, yellow, and orange, respectively. A phosphate group has been modeled on the side chain hydroxyl group of tyrosine 248.

Figure 5: SLAP2 binding precludes LHR-RING interactions with the TKBD

A) Superposition of the Cα atoms of CBL/SLAP2 (PDB id: 6XAR) with CBL TKBD-LHR-RING (PDB id: 2Y1N) and B) TKBD-LHR-RING plus E2 (PDB id: 1FBV). CBL/SLAP2 is shown in dark blue and green, superpositioned on CBL TKBD-LHR-RING shown in beige, yellow, and orange, respectively. E2, pTyr peptide, and calcium ions are shown in cyan, magenta, and mauve, respectively. C) Magnification of the CBL regulatory cleft, with Leu241 of SLAP2 (green) and Tyr371 of CBL LHR (yellow) shown in stick (PDB id: 2Y1N). D) Model depicting CBL autoinhibition and conformational changes induced by phosphorylation of Y371 according to Dou et al.[21], and as a consequence of SLAP/SLAP2 binding. N-terminal regions of SLAP2 are shown in grey or hashed line, as their orientation with respect to CBL and the α-helical C-tail of SLAP2 are unknown.

bioRxiv preprint doi: https://doi.org/10.1101/2020.06.18.159806; this version posted June 18, 2020. The copyright holder for this preprint (which was not certified by peer review) is the author/funder. All rights reserved. No reuse allowed without permission.

Figure 6: SLAP2 relieves CBL autoinhibition *in vitro*

A) *In vitro* ubiquitination reactions containing CBL TKBD-LHR-RING (CBL) or phosphorylated CBL (pCBL), incubated for 100 min with or without SLAP2 or phosphorylated SLAP2 (pSLAP2), analyzed by SDS-PAGE and immunoblotted with anti-ubiquitin antibody. The right panel shows the Fast Green stained PVDF membrane of the transferred reactions. B) As in A, with reactions stopped over a time course of 80 minutes. C) Histogram showing fold change in ubiquitination activity compared to unphosphorylated CBL using E3LITE assay. The pCBL reaction was diluted 2.7 fold to give a comparable detection range on the plate reader. A representative experiment performed in triplicate is shown with error bars representing standard deviation (SD). Biological replicates with independent protein preparations yielded consistent changes in ubiquitination activity and are shown in Supplementary Fig. 4A. D) *In vitro* ubiquitination reactions were analyzed by LC-MS/MS. Stacked histogram of GG-modified ubiquitin K11, K48, and K63 tryptic peptides, shown as a percentage of total signal intensity of the three peptides detected in each reaction. Values were obtained by peak integration of MS1 ion intensity for each peptide. Shown are average values and standard deviations over three independent experiments.

Figure 7: CBL/SLAP2 interface regulates CBL ubiquitination activity

A) *In vitro* ubiquitination reactions containing CBL or pCBL, incubated for 100 min with or without SLAP2 or pSLAP2, WT or mutants (L241R, S244E), analyzed by SDS-PAGE and immunoblotted with anti-Ub antibody. The right panel shows the Fast Green stained PVDF membrane of the transferred reactions. B) Histogram showing fold change in ubiquitination activity in reactions containing CBL and SLAP2 or pSLAP2, WT or mutants, compared to

bioRxiv preprint doi: https://doi.org/10.1101/2020.06.18.159806; this version posted June 18, 2020. The copyright holder for this preprint (which was not certified by peer review) is the author/funder. All rights reserved. No reuse allowed without permission.

unphosphorylated CBL using E3LITE assay. A representative experiment performed in triplicate is shown with error bars representing SD. Biological replicates with independent protein preparations yielded consistent changes in ubiquitination activity and are shown in Supplementary Fig. 4B. C) and D) As in A and B, respectively, comparing CBL WT and *G306E* incubated with SLAP2 or pSLAP2. Biological replicates with independent protein preparations yielded consistent changes in ubiquitination activity and are shown in Supplementary Fig. 4E.

Figure 8: CBL substrate ubiquitination is regulated by the CBL regulatory cleft

A) *In vitro* ubiquitination reactions containing CBL or pCBL WT or mutants (*A223R*, *S226E*, and double mutant *AR/SE*), analyzed by SDS-PAGE and immunoblotted with anti-Ub antibody. The right panel shows the Fast Green stained PVDF membrane of the transferred reactions. B) Histogram showing fold change in ubiquitination activity of CBL mutants compared to unphosphorylated CBL using E3LITE assay. Error bars represent SD. Biological replicates with independent protein preparations yielded consistent changes in ubiquitination activity and are shown in Supplementary Fig. 4F. C) Immobilized GST-CBL or GST-CBL with TKBD mutations *A223R*, *S226E* or *AR/SE*, were incubated with EGFR transfected COS-7 cell protein lysates. Bound proteins were resolved by SDS-PAGE and immunoblotted with anti-EGFR. D) Full length HA-CBL WT or *AR/SE* mutant was co-transfected with FLAG-EGFR and His-Ub in HEK 293T cells. Equivalent protein lysates were resolved by SDS-PAGE and immunoblotted with anti-His to detect ubiquitinated species. Coomassie stain of protein loading is shown. Lysates were probed with anti-FLAG and anti-HA to detect FLAG-EGFR and HA-CBL expression. A representative experiment of biological replicates (n=4) is shown. E) Full length HA-CBL WT or *AR/SE* mutant was co-transfected with FLAG-EGFR and His-Ub in HEK 293T

bioRxiv preprint doi: https://doi.org/10.1101/2020.06.18.159806; this version posted June 18, 2020. The copyright holder for this preprint (which was not certified by peer review) is the author/funder. All rights reserved. No reuse allowed without permission.

cells. EGFR was immunoprecipitated with anti-FLAG, resolved by SDS-PAGE and immunoblotted with anti-His to detect ubiquitinated proteins, anti-FLAG and anti-HA. Expression of transfected EGFR and CBL was detected by anti-FLAG and anti-HA respectively (lower panels). A representative experiment is shown and quantification of biological replicates (n=3) is shown in histogram (F).

bioRxiv preprint doi: https://doi.org/10.1101/2020.06.18.159806; this version posted June 18, 2020. The copyright holder for this preprint (which was not certified by peer review) is the author/funder. All rights reserved. No reuse allowed without permission.

Figure 1

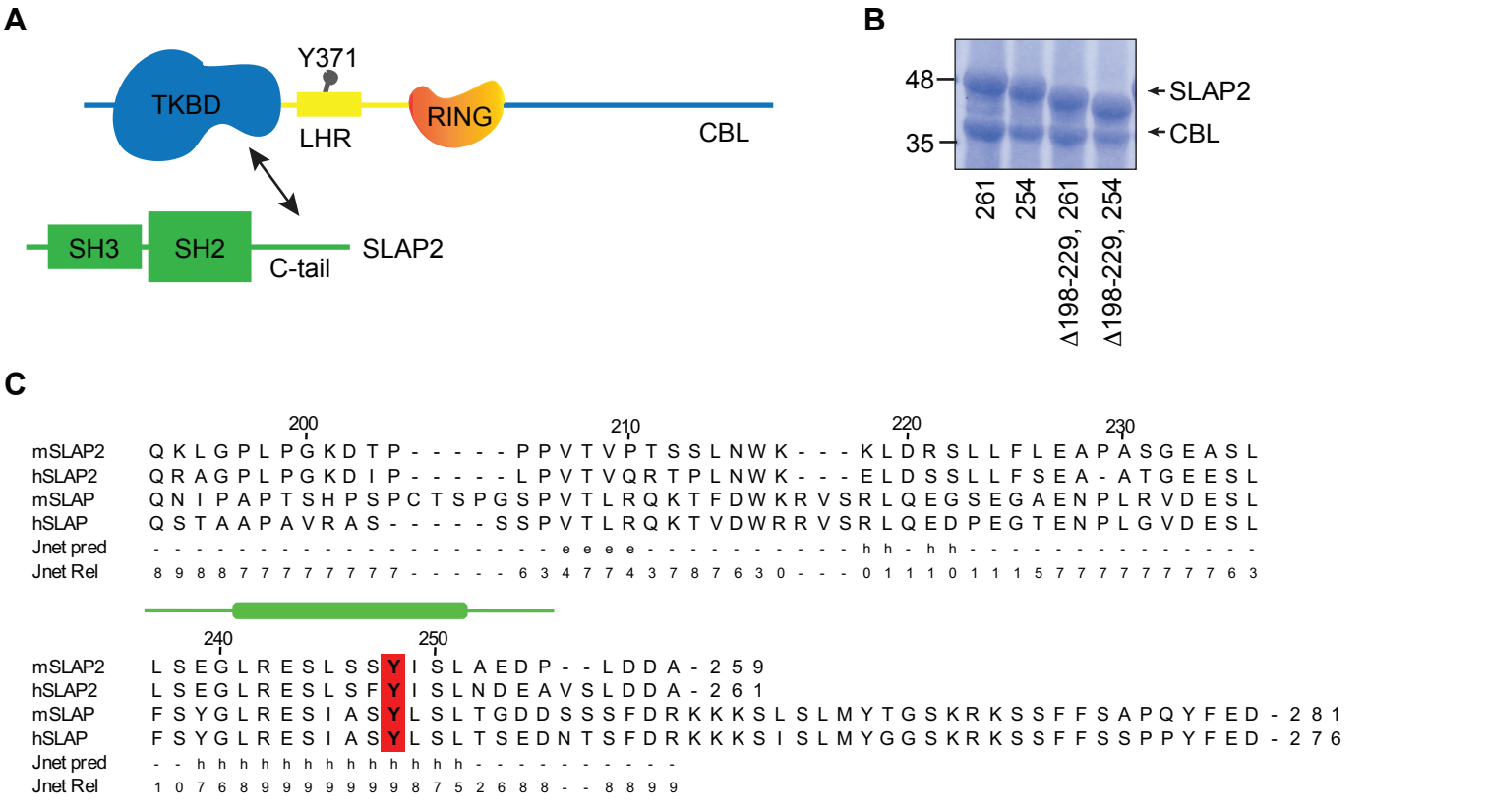

bioRxiv preprint doi: https://doi.org/10.1101/2020.06.18.159806; this version posted June 18, 2020. The copyright holder for this preprint (which was not certified by peer review) is the author/funder. All rights reserved. No reuse allowed without permission.

Figure 2

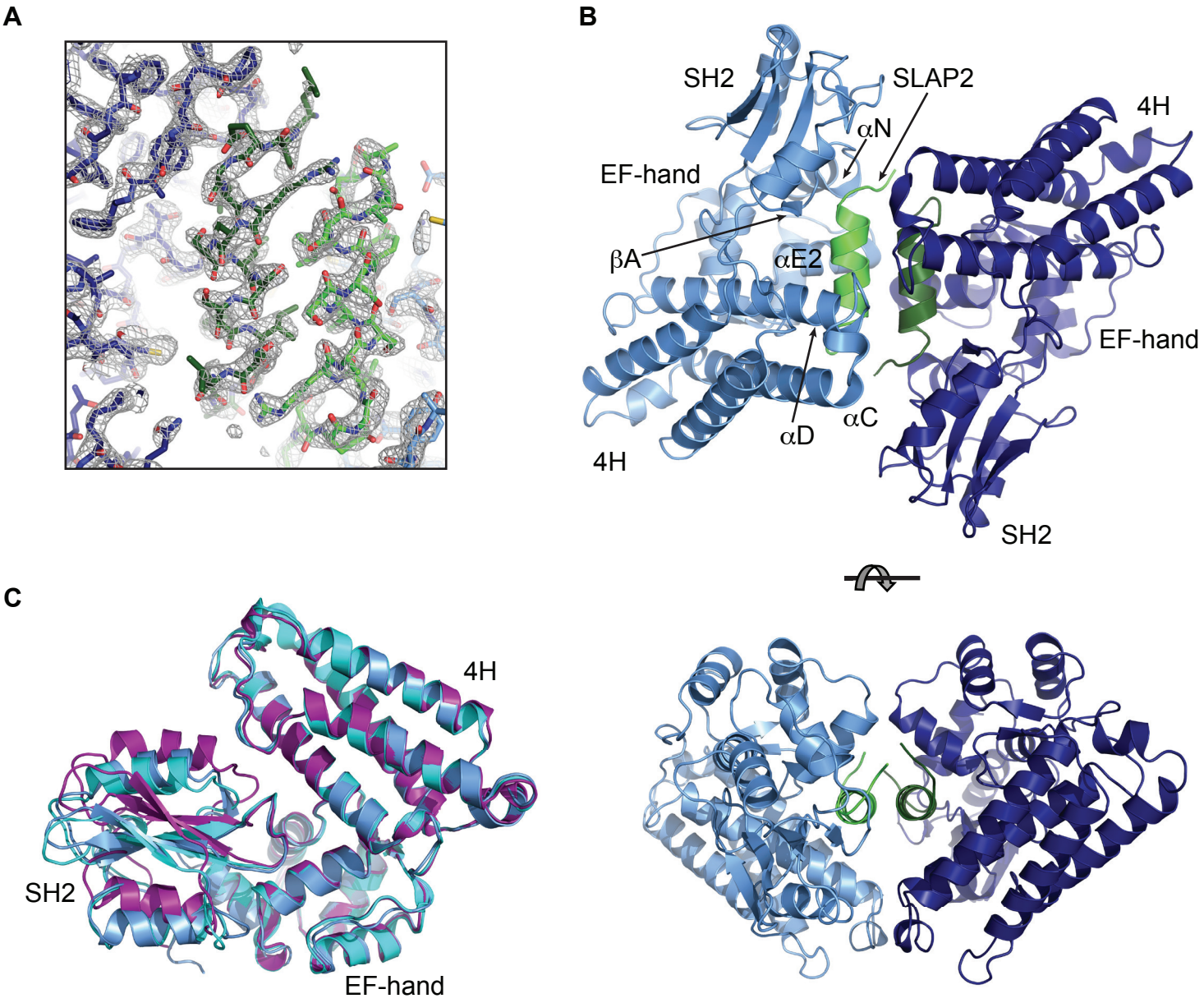

bioRxiv preprint doi: https://doi.org/10.1101/2020.06.18.159806; this version posted June 18, 2020. The copyright holder for this preprint (which was not certified by peer review) is the author/funder. All rights reserved. No reuse allowed without permission.

Figure 3

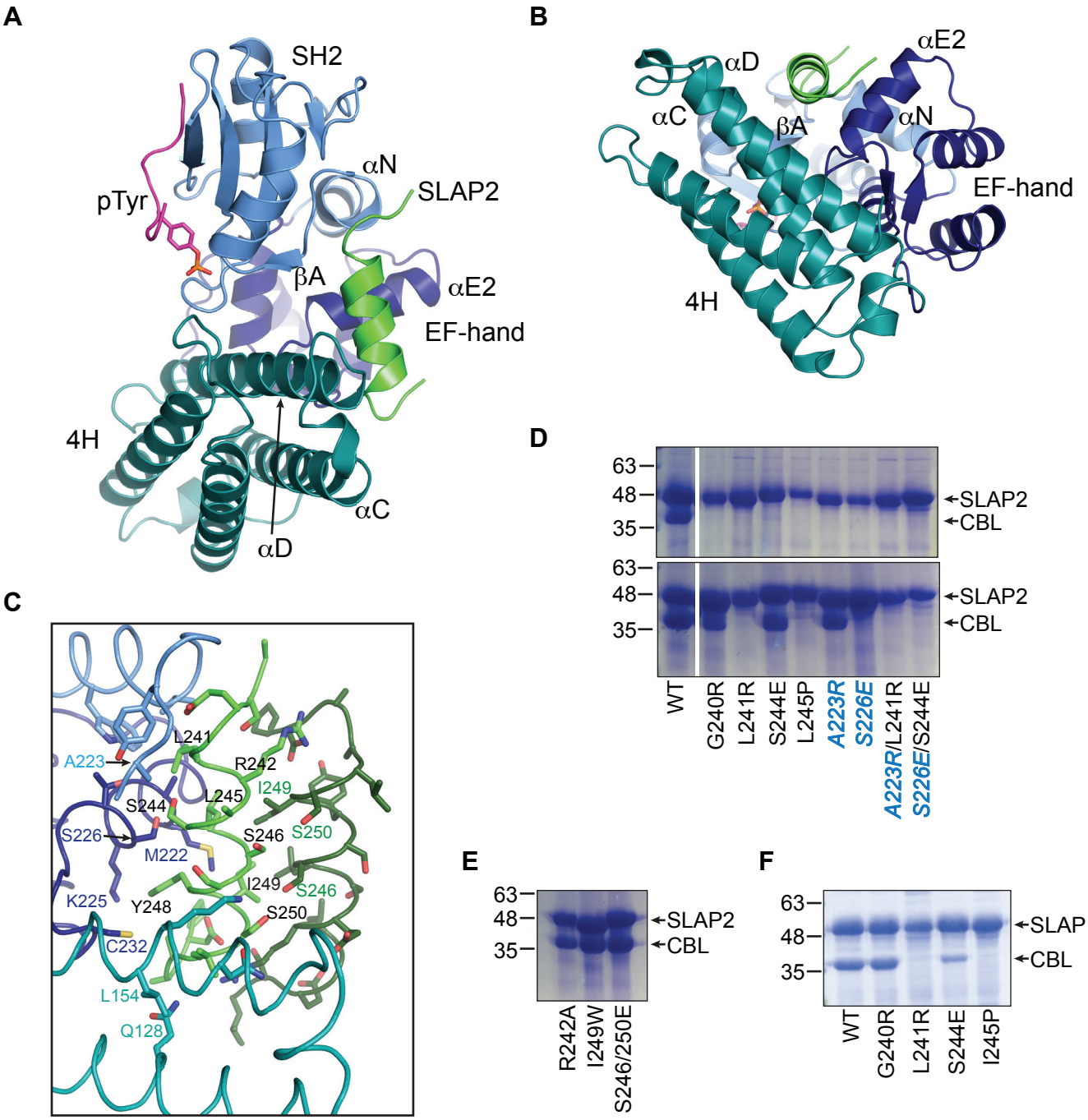

bioRxiv preprint doi: https://doi.org/10.1101/2020.06.18.159806; this version posted June 18, 2020. The copyright holder for this preprint (which was not certified by peer review) is the author/funder. All rights reserved. No reuse allowed without permission.

Figure 4

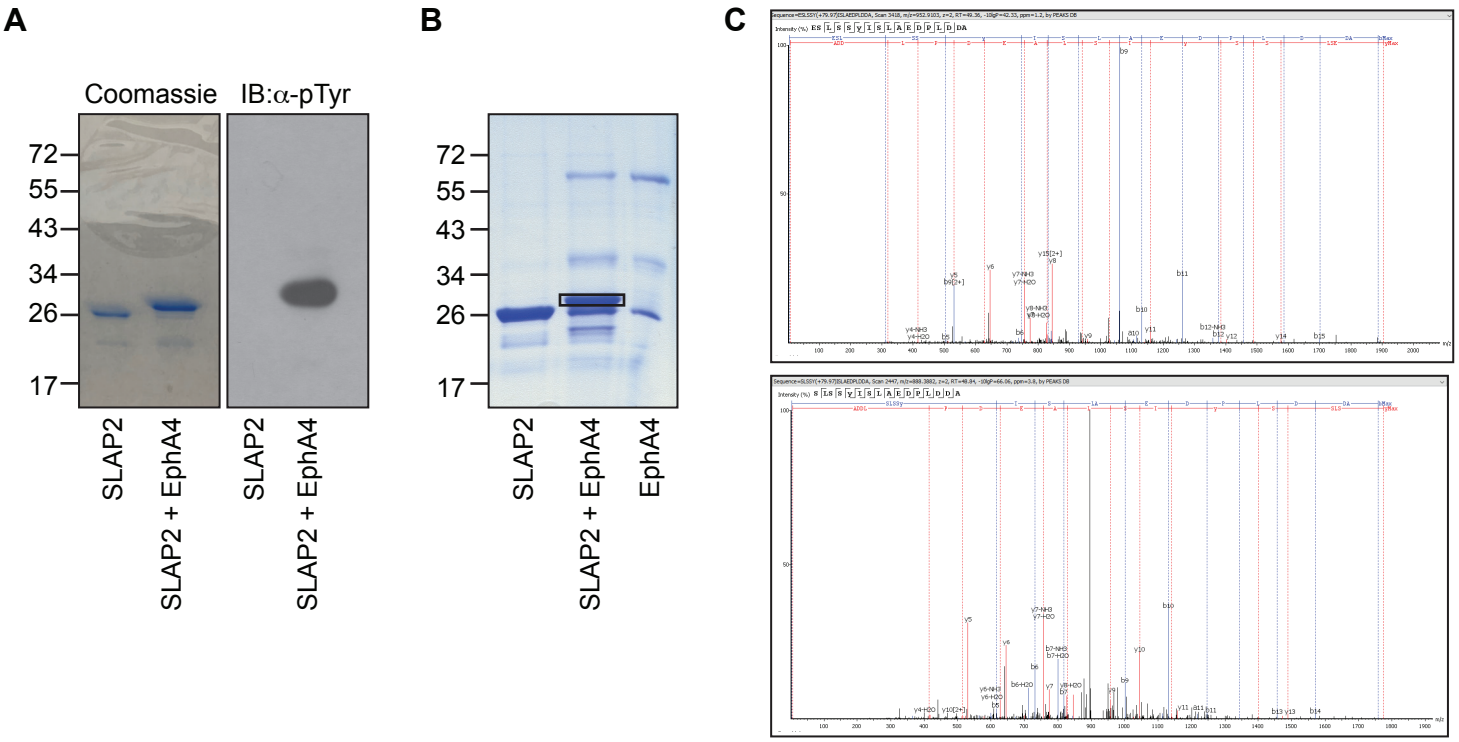

bioRxiv preprint doi: https://doi.org/10.1101/2020.06.18.159806; this version posted June 18, 2020. The copyright holder for this preprint (which was not certified by peer review) is the author/funder. All rights reserved. No reuse allowed without permission.

Figure 5

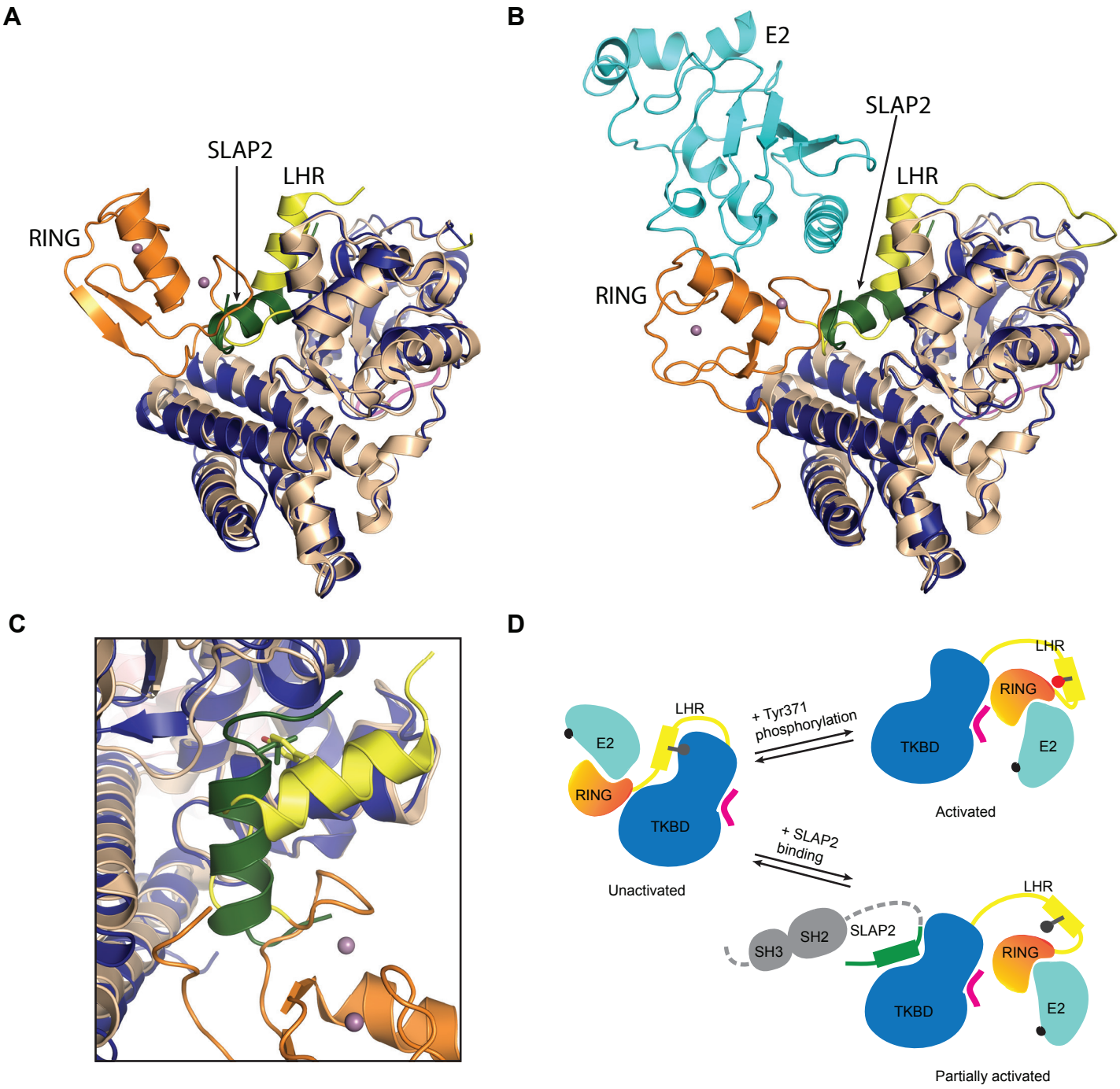

bioRxiv preprint doi: https://doi.org/10.1101/2020.06.18.159806; this version posted June 18, 2020. The copyright holder for this preprint (which was not certified by peer review) is the author/funder. All rights reserved. No reuse allowed without permission.

Figure 6

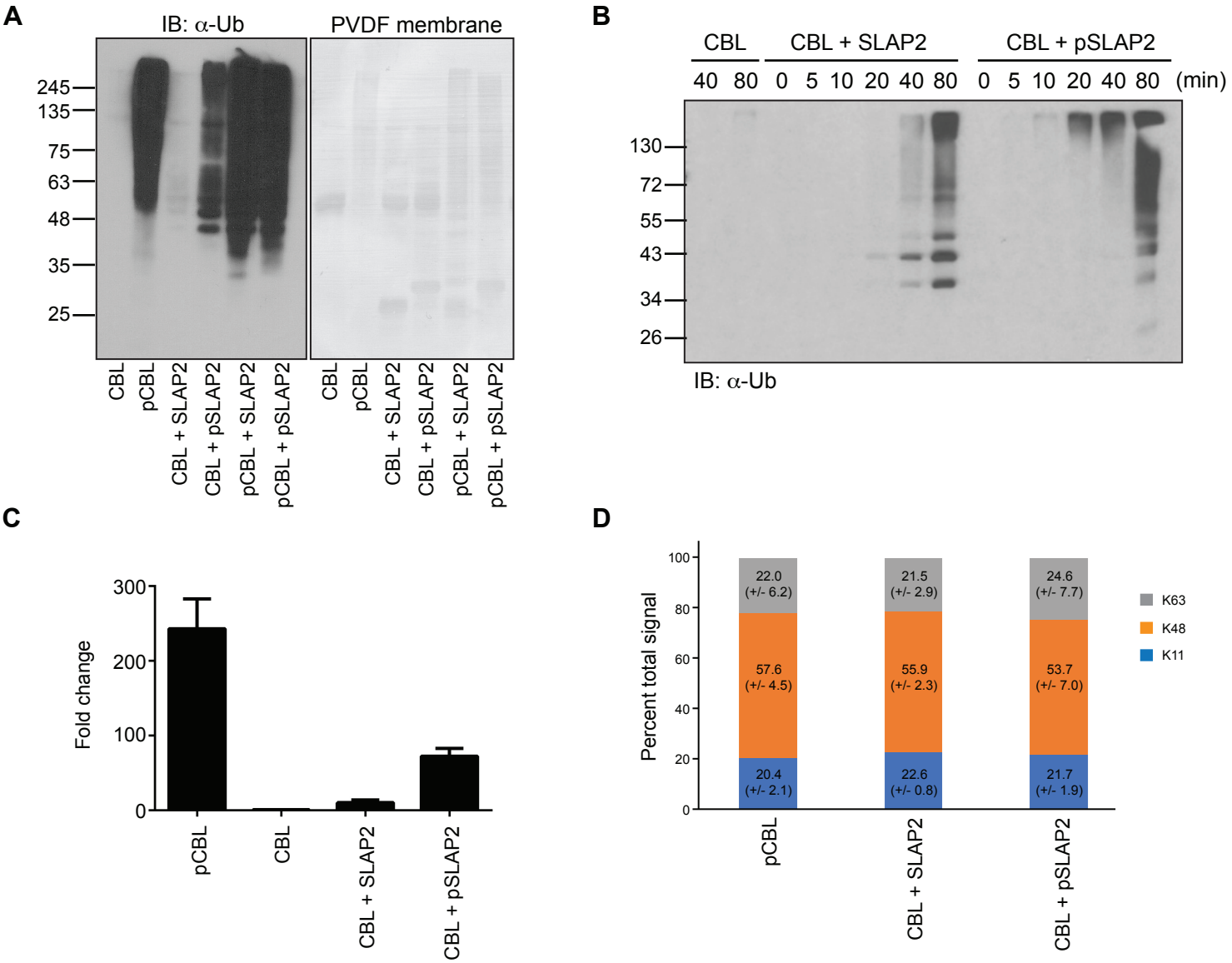

bioRxiv preprint doi: https://doi.org/10.1101/2020.06.18.159806; this version posted June 18, 2020. The copyright holder for this preprint (which was not certified by peer review) is the author/funder. All rights reserved. No reuse allowed without permission.

Figure 7

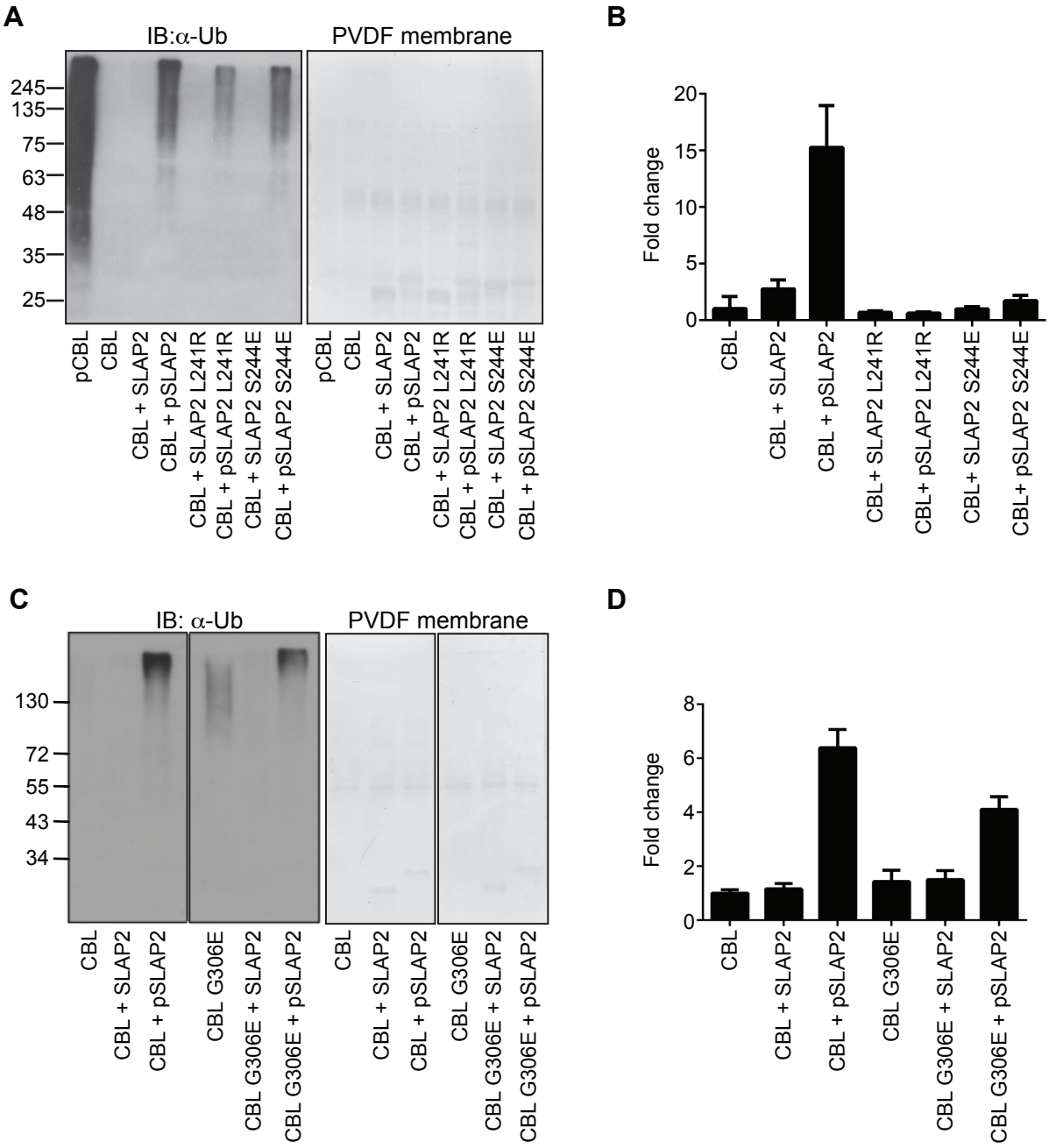

bioRxiv preprint doi: https://doi.org/10.1101/2020.06.18.159806; this version posted June 18, 2020. The copyright holder for this preprint (which was not certified by peer review) is the author/funder. All rights reserved. No reuse allowed without permission.

Figure 8